PERFORMANCE ANALYSIS FOR SINGLE-STAGE AND MULTI-STAGE CORELESS AXIAL FLUX PERMANENT MAGNET GENERATOR WITH DIFFERENT ROTOR STRUCTURES

ASIFUL HABIB

INSTITUTE FOR ADVANCED STUDIES
UNIVERSITY OF MALAYA
KUALA LUMPUR

2020

Universiti Malaya

PERFORMANCE ANALYSIS FOR SINGLE-STAGE AND MULTI-STAGE CORELESS AXIAL FLUX PERMANENT MAGNET GENERATOR WITH DIFFERENT ROTOR STRUCTURES

ASIFUL HABIB

DISSERTATION SUBMITTED IN FULFILMENT OF THE REQUIREMENTS FOR THE DEGREE OF MASTER OF PHILOSOPHY

INSTITUTE FOR ADVANCED STUDIES
UNIVERSITY OF MALAYA
KUALA LUMPUR

2020

Universiti Malaya

UNIVERSITY OF MALAYA
ORIGINAL LITERARY WORK DECLARATION

Name of Candidate: **Asiful Habib**

Matric No: **HGF150001**

Name of Degree: **Master of Philosophy**

Title of Dissertation ("this Work"): **Performance Analysis for Single-Stage and Multi-Stage Coreless Axial Flux Permanent Magnet Generator with Different Rotor Structures**

Field of Study: **Power System Protection**

I do solemnly and sincerely declare that:

(1) I am the sole author/writer of this Work;
(2) This Work is original;
(3) Any use of any work in which copyright exists was done by way of fair dealing and for permitted purposes and any excerpt or extract from, or reference to or reproduction of any copyright work has been disclosed expressly and sufficiently and the title of the Work and its authorship have been acknowledged in this Work;
(4) I do not have any actual knowledge nor do I ought reasonably to know that the making of this work constitutes an infringement of any copyright work;
(5) I hereby assign all and every rights in the copyright to this Work to the University of Malaya ("UM"), who henceforth shall be owner of the copyright in this Work and that any reproduction or use in any form or by any means whatsoever is prohibited without the written consent of UM having been first had and obtained;
(6) I am fully aware that if in the course of making this Work I have infringed any copyright whether intentionally or otherwise, I may be subject to legal action or any other action as may be determined by UM.

Candidate's Signature Date:

Subscribed and solemnly declared before,

Witness's Signature Date:

Name:

Designation:

University of Malaya

PERFORMANCE ANALYSIS FOR SINGLE-STAGE AND MULTI-SATGE CORELESS AXIAL FLUX PERMANENT MAGNET GENERATOR WITH DIFFERENT ROTOR STRUCTURES

ABSTRACT

Axial flux permanent magnet (AFPM) generator is a good candidate for both low and high-speed applications. Compared to radial flux machines, AFPM generators can be easily cascaded for enhanced power/torque while maintaining a fixed machine diameter. To improve power density and reduce cogging torque, some researchers have proposed the removal of iron core in the stator of AFPM machine, giving rise to the concept of coreless AFPM machine. Nevertheless, most of these coreless machines still require back iron on the rotor and/stator to reduce leakage flux. In this project, different rotor structures for single-stage coreless AFPM generators were considered, using two types of magnet arrays: i.e. conventional and Halbach magnet arrays, and two types of rotor materials, i.e. epoxy and iron rotors. The performances of the generators with different rotor structures were evaluated using ANSYS Maxwell® finite element analysis (FEA) software. The results showed that AFPM generator using iron rotor with conventional magnet array gave the overall best performance, even though epoxy rotor with Halbach array demonstrated comparable performance in terms of power density. Based on the findings from the single-stage coreless AFPM generators, the performance of multistage coreless AFPM generators were studied. It was found that by using epoxy rotors with a combination of conventional and Halbach magnet array, a hybrid multi-stage coreless AFPM generator with improved performance can be obtained. Compared to directly cascading multiple single-stage AFPM generators, the multi-stage AFPM generator with hybrid rotor gave better torque density as well as lower torque ripples.

Keywords: Axial flux; fully coreless; permanent magnet generator; Halbach array

ANALISIS PENCAPAIAN UNTUK PENJANA FLUKS PAKSI MAGNET KEKAL TANPA TERAS BERTAHAP TUNGGAL DAN BERTAHAP GANDA DENGAN STRUKTUR PENGGERAK BERBEZA

ABSTRAK

Penjana magnet kekal fluks aksen (AFPM) adalah calon yang baik untuk kedua-dua aplikasi berkelajuan rendah dan berkelajuan tinggi. Berbanding dengan mesin fluks radial, penjana AFPM boleh dengan mudah disalurkan untuk kuasa / tork yang ditingkatkan sambil mengekalkan diameter mesin tetap. Untuk meningkatkan ketumpatan kuasa dan mengurangkan tork cogging, sesetengah penyelidik telah mencadangkan penghapusan teras besi dalam stator mesin AFPM, yang menimbulkan konsep mesin AFPM tanpa teras. Walaubagaimanapun, kebanyakan mesin tanpa teras ini masih memerlukan besi belakang pada pemutar dan / pemegun untuk mengurangkan fluks kebocoran. Di dalam projek ini, beberapa struktur penggerak yang berbeza untuk mesin AFPM tanpa teras bertahap tunggal telah diambilkira, di mana dua jenis susanan magnet, iaitu susunan konvensional dan susunan Halbach, dan dua jenis bahan penggerak, iaitu epoxy dan rotor besi. Pencapaian mesin dengan struktur penggerak yang berbeza ini dinilai dengan menggunakan perisian análisis unsur terhingga ANSYS® Maxwell. Berdasarkan keputusan daripada penjana AFPM tanpa teras bertahap tunggal, pencapaian mesin AFPM tanpa teras bertahap ganda telah dikaji. Dengan menggunakan pengerak epoxy bersama dengan gabungan magnet susunan konvensional dan susunan Halbach, satu mesin AFPM tanpa teras bertahap ganda hybrid dengan pencapaian yang lebih baik dapat diperolehi. Berbanding dengan mesin AFPM bertahap ganda yang diperoleh dengan menggabungkan mesin AFPM bertahap tunggal secara langsung, penjana hybrid ini memberi ketumpatan tork yang lebih tinggi dan riak tork yang lebih rendah.

Kata kunci: fluks berpaksi; tidak benar; penjana magnet kekal; pelbagai Halbach

Universiti Malaya

ACKNOWLEDGEMENTS

My utmost gratitude and solemn subordination to the almighty **Allah Subh'anahu WaTa'ala** for the guidance that He bestowed upon me through all these years of my M. Phil studies.

I express my sincere admiration and thanks to my supervisors **Late Professor Dr. Hew Wooi Ping**, **Dr. Che Hang Seng** and **Professor Dr. Erwan bin Sulaiman** for their brilliant supervision, cordial help, enthusiastic encouragement and kind support. In this connection, I would like to acknowledge the financial support of University of Malaya (UM) to carry out this research work. My sincere thanks go to all the lab and office personnel of UMPEDAC for their assistance and technical support specially Dr. Mahdi Tousizadeh. I earnestly appreciate the special support from a valued brother of mine, **Mr. Mohammed Samir Zoha**.

My deepest gratitude and indebtedness goes to my parents, my sister, my brother and my brother-in-law Dr. Mohammad Rafiqur Rashid for their blessings and the love and support they hold for me all the way. Finally, I must recognize the unwavering and stanch support from my beloved wife and daughter Afifa Asif that kept me steadfast to the goal through all the pains and sufferings throughout this journey. I could not have achieved this much without their assiduous clinch and unremitting love and care.

Universiti Malaya

TABLE OF CONTENTS

Universiti Malaya

Universiti Malaya

Universiti Malaya

LIST OF FIGURES

Universiti Malaya

Universiti Malaya

Universiti Malaya

LIST OF TABLES

Universiti Malaya

LIST OF SYMBOLS AND ABBREVIATIONS

Symbols:

A_m	:	Electrical loading
B_g	:	Magnetic loading
D_{out}	:	Outer diameter
J_a	:	Current density
m	:	Number of phases
K_{pm}	:	PM leakage flux factor
k_s	:	Space utilization factor
K_f	:	Fill factor
l_e	:	Winding length
l_a	:	Pole pair wavelength
l_{act}	:	Active coil length
L_{sc}	:	Coil axial height
N_c	:	Number of turns per coil
N_P	:	Number of parallel strands per conductor
n_{Ml}	:	Number of magnets per wavelength
ρ_{ct}	:	Resistivity of copper
r_{avg}	:	Average radious of the stator winding
S_w	:	Coil cross section area
w_c	:	Width of coil
ω_s	:	Speed
μ_0	:	Permeability of free space
a_P	:	Magnet width to pole pitch ratio
λ	:	Ratio of Inner and outer Diameter

Universiti Malaya

Abbreviations:

AFPM	:	Axial flux permanent magnet generator
C-E Rotor	:	Conventional magnet array with epoxy rotor
C-I Rotor	:	Conventional magnet array with iron rotor
DFIG	:	Doubly fed Induction generator
DSSR	:	Double stator single rotor
H-E Rotor	:	Halbach magnet array with epoxy rotor
H-I Rotor	:	Halbach magnet array with iron rotor
MSMR	:	Multi-stator multi-rotor
NdFeB	:	Neodymium-iron-boron
PMSG	:	Permanent magnet synchronous generator
RF	:	Radial flux
SSDR	:	Single stator double rotor
SSSR	:	Single stator single rotor

Universiti Malaya

CHAPTER 1: INTRODUCTION

1.1 Background

Axial flux permanent magnet (AFPM) machines first appeared in mid 1970s in the technical literature (Campbell, 1974). Soon after, their fields of application spread widely due to their attractive features such as high specific torque at low speed, high efficiency, compact profiles, and flexible topology (Caricchi, 1996; Parviainen, 2005).Their robust structures and compactness make AFPM topologies well suit for high pole machines, high-speed distributed generators (Holmes, 2005), as well as traction motor in electric vehicle (EV) (Yang, 2007).With the use of high-performance rare earth permanent magnet (PM), AFPM machines with high power density can be fabricated(Aydin, 2004).

Design and fabrication of AFPM machine are relatively simple and flexible, because the configuration of both rotor and stator can be altered in many ways (Kahourzade, 2014).Depending on the arrangement of the stator(s) and rotor(s), AFPM machines can be classified as single-stator single-rotor (SSSR), single-stator double-rotor (SSDR) or double-stator single-rotor (DSSR). Among the different AFPM topologies, single-stator double-rotor (SSDR), also known as two-outer-rotors-unitary-stator(TORUS), configuration is usually preferred for its high efficiency, mechanical strength and power density (Kahourzade et al., 2014).

Universiti Malaya

Figure 1.1: Relative positions of the stator(s) and rotor(s)for SSSR, DSSR, SSDR and MSMR

One of the key advantages of the AFPM machine is the ease to increase the power of the machine without increasing diameter of the machine (Javadi& Mirsalim, 2008; Kahourzade et al., 2014). This can be done by cascading multiple single-stage AFPM machines, which can be either DSSR or SSDR (Caricchi et al., 1996), into multi-stage AFPM machine that have multi-stator-multi-rotor (MSMR) structure. The relative positions of the stator(s) and rotor(s) for SSSR, DSSR, SSDR and MSMR are shown in Figure 1.1. Ship propulsions, aircraft propulsions, pumps, wind energy generation, low and high speed PM generators are some of the application that can benefit from multistage AFPM machines (Caricchi et al., 1994).

Both single-stage and multi-stage AFPM machines can be further classified based on the design and material of the stator, i.e. slotted or slot less, with iron core or ironless/coreless (Javadi & Mirsalim, 2008). Among these, coreless AFPM machine is an interesting type of AFPM machine that has been successfully employed since the last two decades. Coreless AFPM machines have some noticeable advantages compared to conventional AFPM machines with iron core, such as higher power/torque densities, torque-to-weight ratios, and geometrically higher aspect ratios (Aydin & Gulec, 2016). Being coreless, the machine does not experience eddy current (hence, no hysteresis losses) and has lower cogging torque. This allows the machine to run at higher efficiency compared to other conventional machines (Javadi & Mirsalim, 2008).Moreover, the coreless structure reduces the weight of the machine making it significantly more portable (Schumann, 2014). In the literature, coreless AFPM machine usually refers to stator coreless where the stator core is replaced by non-ferrous material such as epoxy, but ferromagnetic structure (i.e. back-iron) is still used in the rotor. A fully coreless design, wherein both rotor and stator use non-magnetic materials, will further reduce the machine weight as well as material and fabrication cost. In addition, mechanical stress also reduces as the machine does not produce attractive forces between the two non-metallic rotors and stator except between the permanent magnets on the rotors.

However, removing the rotor back-iron will result in significant flux leakage on the back surface of the rotor and deteriorate the performance of the machine. So special considerations need to be made, such as the use of Halbach array, while the conventional magnet arrangement provides two-sided magnetic field, the Halbach array creates a single-sided magnetic field, by canceling the flux on one side and amplifying the flux on the other side as shown in Figure 1.2. Several works on the use of Halbach array for AFPM has been presented in (Lee et al., 2004; Praveen et al., 2012; QI et al., 2006; Zhu et al., 2013; Zhu & Howe, 2001).This feature of Halbach array can be extended to the coreless AFPM machine without rotor back-iron to handle the leakage flux problem.

Universiti Malaya

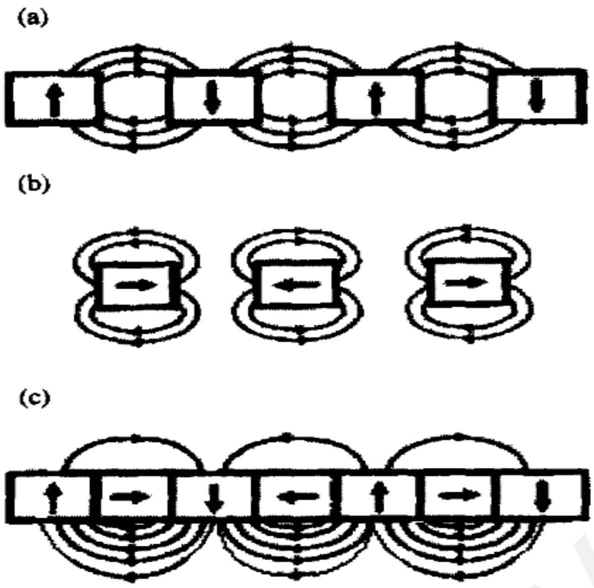

Figure 1.2: Halbach Array formation (Wang et al., 2006)

1.2 Problem Statement

Previous works on coreless AFPM generator have been focusing on “stator coreless” machine, where the iron-core in stator has been replaced with non-ferrous materials but the rotor still retaining its back iron. Theoretically, the rotor back-iron can also be replaced by non-ferrous material to yield a so-called fully coreless machine that can be lighter and has potentially better power/torque density. Furthermore, the removal of rotor back iron can open the opportunity for additive manufacturing of such machines, using 3D printers that are increasingly accessible.

However, research works towards achieving such fully coreless structure for AFPM machine are very rare and there is little understanding on how such machine performs compared to conventional coreless AFPM machines with iron rotor. In addition, simply removing the rotor back iron is likely to increase the leakage flux and reduce the performance of the machine. Thus, to obtain reasonable performance from such fully coreless machine, the use of specialized magnet arrays, such as Halbach array, could be a potential option. To the best of the candidate’s knowledge, comparative study on the performance of coreless AFPM generator with rotor that uses epoxy structure and

Halbach array with conventional generators using iron rotor and normal magnet arrays is yet to be reported.

When cascading multiple single-stage coreless AFPM generators to form multi-stage coreless AFPM generator, the multi-stator and multi-rotor structure opens opportunities for more innovative design. The idea of having non-ferrous rotor structure can be extended from single-stage to multi-stage coreless AFPM generator. It is interesting to note that the Halbach array will not be needed for the inner rotors since the cancelling of magnetic field on one side of the rotor is not required. This provides the possibility to combine conventional magnet array with Halbach magnet array to form a multi-stage coreless AFPM generator with hybrid rotor structure. Since such machine has not been introduced in the past, a study on its performance will be necessary to determine the potential merits compared to conventional multi-stage AFPM generators.

1.3 Objectives of the Research

Based on the problem statement, the objectives of this research can be enumerated as follows:

1. To develop simulation model for a single-stage and multi-stage coreless AFPM generator using ANSYS Maxwell finite element analysis software.
2. To evaluate the performance of single-stage coreless AFPM generators with different rotor structures by altering the type of magnet array (conventional and Halbach) and rotor materials (iron and epoxy).
3. To evaluate the performance of multi-stage coreless AFPM generators with hybrid rotor structures.

Universiti Malaya

1.4 Research Questions

This project is undertaken to answer the two following research questions:

1. How is the performance of single-stage coreless AFPM generator with epoxy rotor and Halbach magnet array when compared to the same generator using iron rotor and conventional magnet array?
2. How is the performance of multi-stage coreless AFPM generator with epoxy rotor using a combination of conventional and Halbach magnet arrays when compared to similar generator obtained by directly cascading multiple single-stage coreless AFPM generators?

1.5 Research Gaps and Contributions

The research gaps addressed by this project and the corresponding contributions are listed in the Table 1.1

Table 1.1: Research gap vs. contribution

No	Research Gap	Contribution
1	Comparison of single-stage coreless AFPM generators with different rotor structure which utilizes different magnet arrays and rotor materials	While coreless AFPM generator with iron rotor and conventional magnet array still give the best performance, using epoxy rotor and Halbach magnet array can provide comparable performance in terms of torque density.
2	Comparison of multi-stage coreless AFPM generator obtained by directly cascading multiple single-stage coreless AFPM generators with fully coreless AFPM generator using epoxy rotor with hybrid magnet arrays	It has been demonstrated that hybrid multi-stage coreless AFPM generator proposed in this project provides better performance than direct-cascaded multi-stage AFPM generator, where reduced axial thickness, lower torque ripple with higher torque density were obtained.

Universiti Malaya

1.6 Scope of the Research

The scopes of this research work are explained as follows:

1. The study on machine performance in this project is based on finite element analysis (FEA) simulation only. Fabrication and experimental testing of the machines discussed in this project is beyond the scope of this work. Industrial grade FEA software, i.e. ANSYS® Maxwell, has been utilized to ensure accurate results that reflect actual performance of the machine can be simulated.
2. For objective 2, the focus is on performance comparison between single-stage coreless AFPM generators with different rotor structure. Since two types of magnet arrays (conventional and Halbach) and two types of rotor materials (iron and epoxy) are considered in this project, four different rotor structures are included for comparison, i.e. conventional-iron (CI), conventional-epoxy (CE), Halbach-iron (HI) and Halbach-epoxy (HE).
3. For objective 3, when evaluating the performance of multi-stage coreless AFPM generator only the best performing single-stage coreless AFPM generator, i.e. the generator with CI rotor, is used as the reference for comparison.
4. To ensure fair comparison between the different AFPM generators, the same stator structure is used for all the AFPMs and only the rotor design is modified. Furthermore, the same rotor diameter and same magnet volume are maintained for all AFPM generators.
5. The project does not include any optimization of machine parameters.

Universiti Malaya

1.7 Organization of the Thesis

The findings obtained from this research project are reported in thesis, where its contents are distributed over six chapters. **Chapter 1** gives a general introduction along with problem statement, research questions, research objectives and scope of the study. The rest of the chapters are organized as follows:

Chapter 2: This chapter is the summary of the previous literature about the axial flux and coreless axial flux permanent magnet machine and also the summary of conventional and Halbach magnet arrangements used in AFPM machine. This chapter is concluded with a summary of the research gap.

Chapter 3: The detail research methodology is presented, where analytical equations used for designing the AFPM machines are explained and simulation tools (i.e. Ansys Maxwell) are discussed. The whole design process has been described step by step in this chapter. Modelling of single-stage coreless AFPM generator and multi-stage coreless AFPM generator also discussed in this chapter.

Chapter 4: The simulation results of single-stage coreless AFPM generator along with corresponding explanation behind have been discussed in this chapter. The findings from the comparison of air-gap magnetic flux density, torque and torque ripple, power and power density of the four different generators are detailed in this chapter.

Chapter 5: The simulation results of multi-stage coreless AFPM generator, along with corresponding explanation, have been presented in this chapter. The comparison of air-gap magnetic flux density, torque and torque ripple, power and power density of the proposed 'hybrid multi-stage coreless AFPM generator' with direct cascade multi-stage coreless AFPM generator are discussed in this chapter.

Universiti Malaya

Chapter 6: The chapter wraps up the thesis with some concluding remarks and recommendations for future works.

Universiti Malaya

CHAPTER 2: LITERATURE REVIEW

2.1 Introduction

This chapter presents an overview on previous research works related to the project, based on peer-reviewed journal papers, specialized conference articles, thesis reports, internet sources, and personal communications with the experts both from industry and academia. An introduction on the AFPM machine including its history, working principle and advantages over other permanent magnet (PM) machines is delivered at the inception of the chapter. Chronological overview on the previous research works related to AFPM machine is briefly enumerated with pertinent implications. Since this research focuses on coreless AFPM, the concept of coreless AFPM along with an introduction to the Halbach and conventional array with their implementation in the present research have also been discussed. Finally, a summary of the literature review is provided at the end of the chapter to relate the research gaps identified with this project.

2.2 Axial Flux Permanent Magnet (AFPM) Machine

The first electrical generator, invented by Michael Faraday in 1831(Howard, 1967), had an axial-flux orientation which produced DC current by a copper disk while rotating in an axial field. However, this concept of axial orientation did not get that much endorsement that time (Martin, 2007). On the other hand, radial-flux machines, which was developed by Thomas Davenport, ruled the market upto1970s (Davenport, 1837). Then again, in late 1970s, the axial flux machines revived through the works of Campbell and became practical for commercial applications (Campbell, 1974).

In contrast to the conventional radial flux machines, flux in AFPM machine propagates axially (i.e., along the axis of the output shaft) through the air gap between

Universiti Malaya

the rotor and the stator in axial-flux machine. Figure 2.1 shows the flux orientation of axial and radial flux machines. As can be seen from the figure, the rotor of axial-flux machine has a pancake or disk-like structure, with typically higher diameter to axial length ratio than the radial flux machines (Gieras et al., 2008).

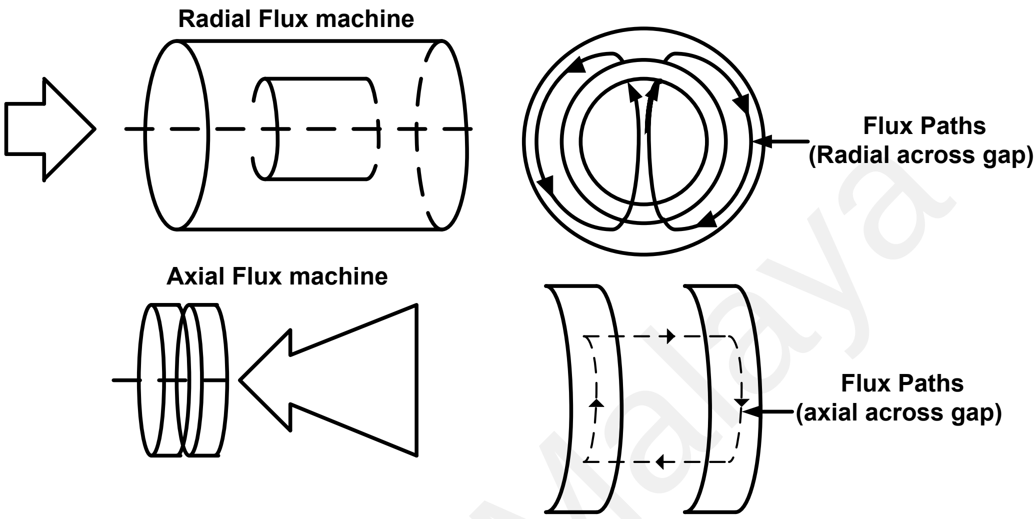

Figure 2.1:Basic flux orientation comparison between axial and radial flux (Martin, 2007)

The increased availability of more powerful permanent magnets (such as neodymium-iron-boron, NdFeB) has spurred research on AFPM machines in the last couple of decades. Moreover, the benign features of axial-flux machines over the radial-flux ones, e.g. higher power density, flexibility in field and winding design, better cooling, possibility of cascaded system, robustness and compactness of structure and short axial length, make them more attractive to the researchers (Chan et al., 2010).

All these desirable features of AFPM machines lead to new range of applications like electric vehicles, portable generators and mobile battery charger (Wang et al., 2011). Furthermore, the axial structure of AFPM machine allows the number of poles to be increase easily compared to radial flux machine, making AFPM favourable in low speed application such as wind turbine.

Universiti Malaya

2.2.1 AFPM Machine Topologies

The AFPM machine topologies can be classified from different viewpoints. Considering permanent magnet position in the rotor, it can be classified into PM interior rotor and PM external rotor; considering the presence of armature core and slots, it is classified as with or without armature slots and with or without armature core. AFPM machines can be designed with different number of rotor and stator. Considering the number of rotor and stator parts in the machine, it can be classified as single-sided, double-sided and multistage machine. Single sided AFPM machine in the form of one stator and one rotor construction named single-stator single-rotor (SSSR) topology (Khan et al., 2019). The double-sided topology can be formed by two different combination of rotor and stator, viz., single-stator double-rotor (SSDR) and double-stator single-rotor (DSSR). Single sided structure has an advantage of using less PMs which is applicable for the low cost AFPM machines. On the other hand, double sided and multistage AFPM machine have the advantage of higher power density with same diameter of the machine (Gieras et al., 2008; Kahourzade et al., 2014). The classification of AFPM topologies based on rotor and stator structure is shown in Figure 2.2 and briefly described in subsequent sections.

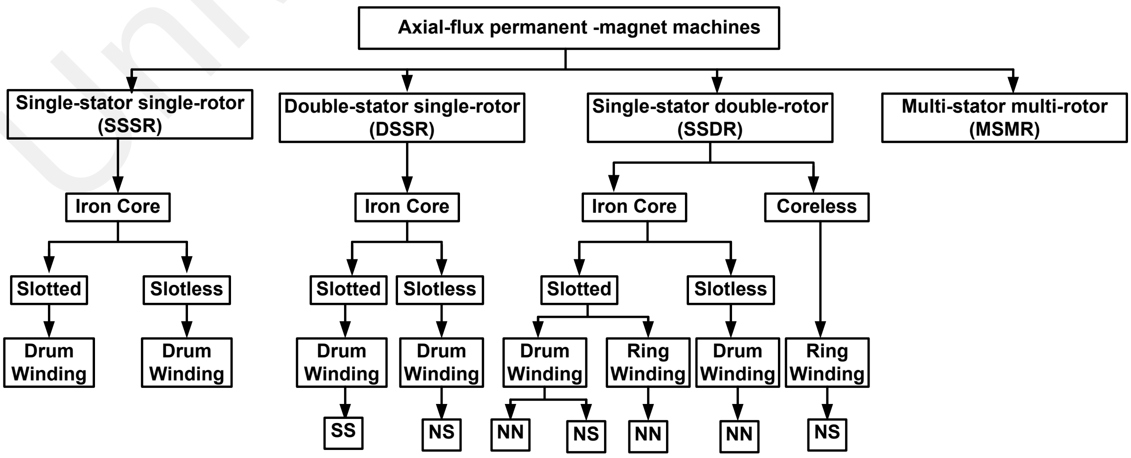

Figure 2.2: Various topologies of AFPM machine
(Kahourzade et al., 2014)

Universiti Malaya

2.2.1.1 Single-sided AFPM machine

For single-sided AFPM machine, only one combination is possible, which is single-stator single-rotor (SSSR) (Figure 2.3). Its structure very simple with only one single-stator and single-rotor, the stator windings chiefly non-overlapping (though distributed windings are also employed). The advantages of SSSR lie in its compact structure and high torque capability; hence, it is employed in industrial traction, servo electromechanical drives, military, transportation industries and gearless elevators, etc. The major demerit of SSSR is that there are possibilities of imbalance axial force between stator and rotor, which may twist the structure easily (Gieras et al., 2008; Kahourzade et al., 2014).

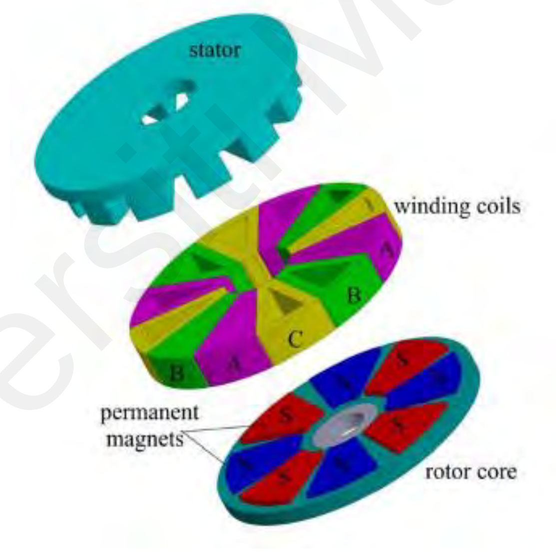

Figure 2.3:3D view of SSSR AFPM machine
(Kahourzade et al., 2014)

2.2.1.2 Double-sided AFPM machine

For double-sided AFPM machine, two combinations are typically available, single-stator double-rotor (SSDR) and double-stator single-rotor (DSSR). These types of AFPM structure are known as the sandwich structure.

(a) **SSDR topology:**

In SSDR the stator is sandwiched between two external rotors. In this structure, the stator can be slotted or slot less and coreless. Single layer concentrated winding is common for this topology. In slotted SSDR (Figure 2.4 (a)), the flux travels axially through the stator or circumferentially in the stator core and torque is generated in radial directed windings (Huang et al., 2001). In slot less topology, less copper loss can be achieved due to shorten end windings as a result of less leakage and mutual inductance. Therefore, flux ripple, cogging torque and rotor loss can be eliminated. Flux path for slotted SSDR AFPM machine can be achieved in two ways: NN type and NS type (Kahourzade et al., 2014).

Another type for SSDR AFPM machine comes in the form of coreless (Figure 2.4 (b)) concept. In coreless SSDR AFPM machine, the main flux travels from one external rotor to another external rotor along the stator windings. Windings are mounted only on the stator, while the rotor contains surface mounted permanent magnets. Coreless topology offers high efficiency with less cogging torque and higher power density (Kahourzade et al., 2014).

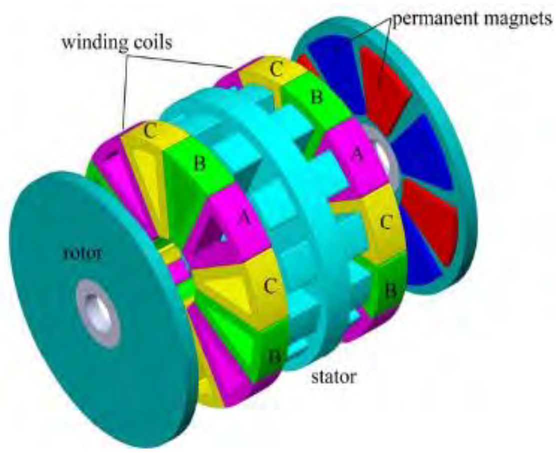

(a)

Figure 2.4: (a) 3D view of slotted SSDR (b) 2D view of coreless NS type SSDR topology
(Kahourzade et al., 2014)

Universiti Malaya

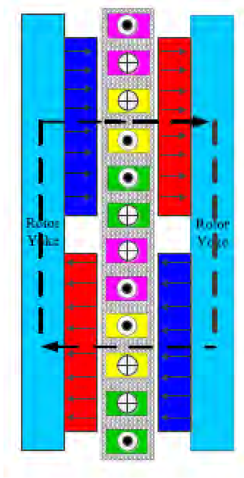

(b)

Figure 2.4, continued

(b) **DSSR topology:**

In this topology, the rotor is sandwiched between two external stators. Like SSDR AFPM machine, DSSR topology can also be either slotted stators (SS type) or slotless stators (NS type) (Parviainen et al., 2004). Both surface mounted and buried PM can be attached to the rotor discs. Figure 2.5 shows the 3D view of a DSSR AFPM machine. The flux travels axially and circumferentially for surface mounted and buried magnet configuration, respectively. Despite of having some advantage (like protection of magnets against mechanical impact, corrosion, etc.) buried magnet configuration offers less power density than that of surface mounted PM rotor. On the other hand, leakage flux of PM is not higher as the PM is surrounded by the ferromagnetic material (Aydin et al., 2006)

In another DSSR topology, iron rotor disc is replaced by non- ferromagnetic material which facilitates high power density due to reduced weight. This kind of topology mainly applicable for small inertia applications. DSSR topology suffers from higher copper loss than any other topology of AFPM machine due to long end windings.

Universiti Malaya

Hence, non-magnetic material such as epoxy is suggested for improving the compactness of DSSR structure and heat transfer as well (Caricchi et al., 1998).

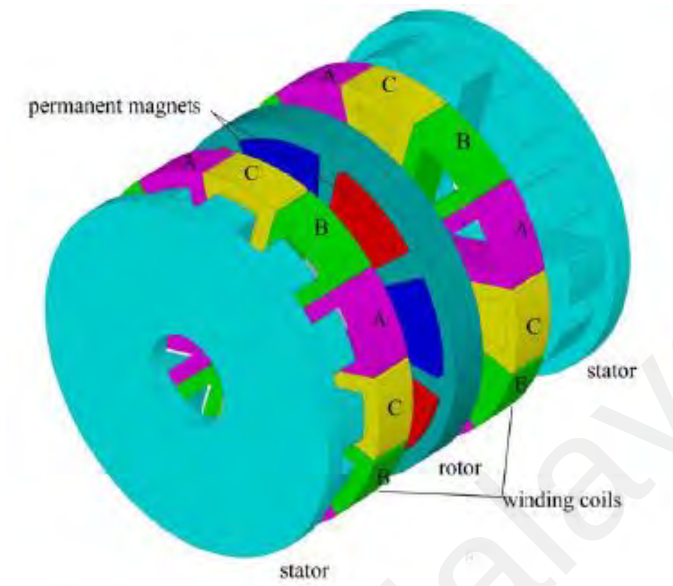

Figure 2.5: 3D view of DSSR topology
(Kahourzade et al., 2014)

2.2.1.3 Multi-stage AFPM machine

It is possible to obtain multi-stage, also known as multi-stator multi-rotor (MSMR), AFPM machine by extending the double-stator single-rotor (DSSR) or single stator double rotor (SSDR) configurations. Generally, direct cascade approach is the most natural approach to obatin the AFPM machines, where multiple AFPM machines share a common shaft to achieve higher power/torque performance. With the same mechanical shaft, the multi-stage SSDR machine will have N stators and N+1 rotors, while the multi-stage DSSR machine will have N+1 stators and N rotors(Kahourzade et al., 2014).Multi-stage AFPM machines are easy to construct because of their planar structure; moreover, multi-stage configuration enhances the torque and power density without increasing the machine diameter.

All the topologies of single-stage structures may form multi-stage structure simply by cascading several single-stage AFPM machines together. For example, slotted or slotless, iron core or coreless, NN or NS topologies can be augmented in multi-stage configuration (Kahourzade et al., 2014). The other merits and demerits of the above-mentioned topologies resemble much with their corresponding single-stage structures. The multistage AFPM machines have found their applications in ship propulsions, pumps, and high-speed PM generators (Caricchi et al., 1994). Figure 2.6 shows a 3D view of a multi-stage topology of an AFPM machine.

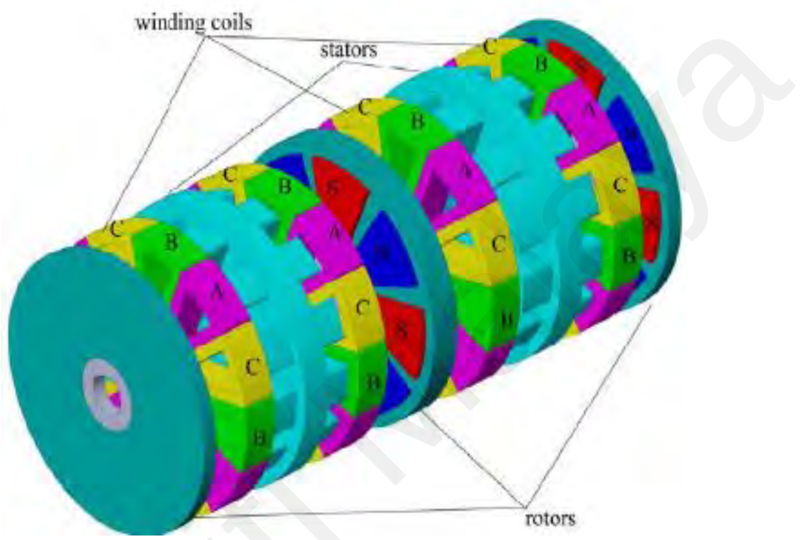

Figure 2.6: 3D view of a multi-stage topology
(Kahourzade et al., 2014)

2.3 Coreless AFPM Machines

A coreless machine is the one in which winding area of the stator do not contain ferromagnetic material or iron core, but only consists of air or nonmagnetic material. This type of AFPM was first introduced a couple of decades ago and since then it has gained much recognition because of its many advantageous features over conventional AFPM with iron core. Firstly, iron loss and cogging torque can easily be avoided in coreless machines, which gives higher efficiency and low vibration (Javadi & Mirsalim, 2008; Rossouw, 2009). Besides, magnetic losses in coreless machines are negligible, that is why iron rotor disk can be used to build coreless machines (Chirca et al., 2014). Furthermore, due to large volume of permanent magnets coreless stator can produce very high torque. Figure 2.7 and Figure 2.8 show the basic structures of a coreless AFPM machines.

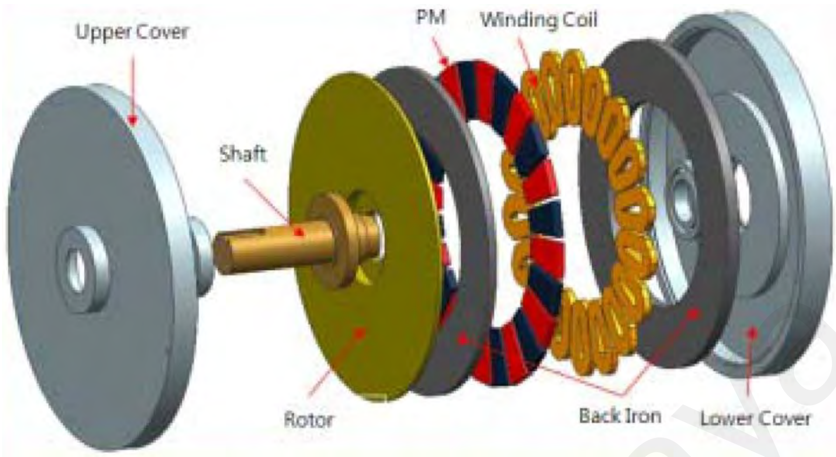

Figure 2.7: Basic structure of coreless AFPM machine
(Chung & You, 2014)

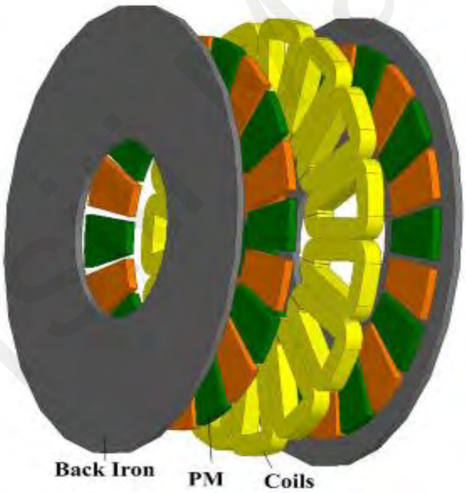

Figure 2.8: Basic structure of coreless AFPM machine (double rotor)
(Xia et al., 2015)

In (Xia et al., 2015), a comparative study have been carried out for air cored AFPM machine with different stator winding configurations. For a double sided coreless stator axial flux permanent magnet micro wind power has analyzed in (Chirca et al., 2014). In (Daghigh et al., 2015) designed coreless AFPM synchronous generator at low material cost. A discussion about analysis and performance of AFPM using non overlapping concentrated winding have done in (Kamper et al., 2008). In (Lee et al., 2015) evaluated the performance of coreless AFPM wind generator. An eddy current loss calculation for coreless axial flux permanent magnet machine was calculate in (Wang & Kamper, 2004). An analytical magnetic field analyses as well as back electromotive force were calculated in (Virtic et al., 2008) for a coreless axial flux permanent magnet generator. In (Wang et al., 2011) analyze by supplying a rectifier load to the coreless axial flux permanent magnet generator.

A coreless AFPM generator has been designed for automotive application wherein the stator part was coreless and the rotor was made from ferromagnetic material (Javadi & Mirsalim, 2008). In (Javadi & Mirsalim, 2010)steel back plates has been used for two coreless stators in designing a 42-V coreless AFPM generator for automotive application. In (Tan et al., 2015) different winding configurations for an air cored AFPM machine has been studied where only the stator part was coreless. In (Minaz & Çelebi, 2017) design and analysis of a new axial flux coreless PMSG has been carried out wherein the two stators were coreless against three iron rotor disk. The stator part was only coreless for high-speed AFPM generator in determining the rotor yoke thickness (Sadeghierad et al., 2009). In an analytical analysis of the magnetic field and back electromotive force only the coreless stator was considered in an AFPM generator (Virtic et al., 2008).

Non-ferromagnetic stator and ferromagnetic rotor have used to construct an axial-flux coreless permanent magnet generator at relatively low cost (Hosseini et al., 2008). On the other hand, a high speed coreless AFPM generator design is presented in (Fei et al., 2010). Where coreless stator and mild steel rotor is attached with aluminum holders. Plastic structure has been used for the rotor to design a light weight high speed axial-flux machine for aircraft drive where iron ring was used only for flux path closure (Eastham et al., 2002).

From the literature reviewed, it can be concluded that the coreless AFPM machines reported so far are only having coreless stator while retaining the ferromagnetic rotor

Universiti Malaya

structure. Hence, technically speaking, the coreless AFPM machines in the literature are only stator coreless but not fully coreless.

Naturally, a fully coreless design offers less weight and low cost and improves mechanical strength of the structure as the machine does not produce any attaractive force between the two rotors and stator except the two opposite of PMs attached with the epoxy rotor. On the other hand, iron-rotor conventional array with an optimized magnet-width to pole-pitch ratio produces higher torque than the iron-rotor and epoxy rotor Halbach array up to a certain thickness of magnets (Ofori-Tenkorrang & Lang, 1995). When the performance of epoxy rotor conventional array is compared that with epoxy rotor Halbach array for any thickness of magnet the later is always found to produce higher torque. So a resonable solutions for larger torque for epoxy rotor are double or tripple disc machine (Ofori-Tenkorrang & Lang, 1995). Consequently, a full performace comparison among the conventional feromagnetic and non-feromagnetic rotor machines and Halbach feromagnetic and non feromagnetic rotor machines have been carried out in the present research.

2.4 Conventional and Halbach Magnet Array

The arrangement of magnets is an important design criterion for AFPM machine, and two arrangements can be considered for AFPM machine: the conventional array and the Halbach array. For conventional array, the magnets are arranged with alternating north and south poles, either in radial (Figure 2.9(a)) or tangential direction (Figure 2.9(b)). The Halbach array can be considered as a combination of two conventional arrays (radial and tangential), as illustrated in Figure 2.9(c). The arrangement of the magnet poles in Halbach array helps to strengthen the field in one side of the array while canceling out the field on the other side (Figure 2.9(d)) (Zhu et al., 2013). An AFPM machines employing Halbach array has several advantages over a standard AFPM machine, as follows (Gieras et al., 2008; Halbach, 1981, 1985):

- The fundamental field is stronger by a factor of 1.4 than in a conventional PM array, and thus the power efficiency of the machine is approximately doubled.
- The array of PMs does not require any backing steel magnetic circuit and PMs can be bonded directly to a non-ferromagnetic supporting structure (aluminium, plastics).
- The magnetic field is more sinusoidal than that of a conventional PM array; Halbach array has very low back-side fields.

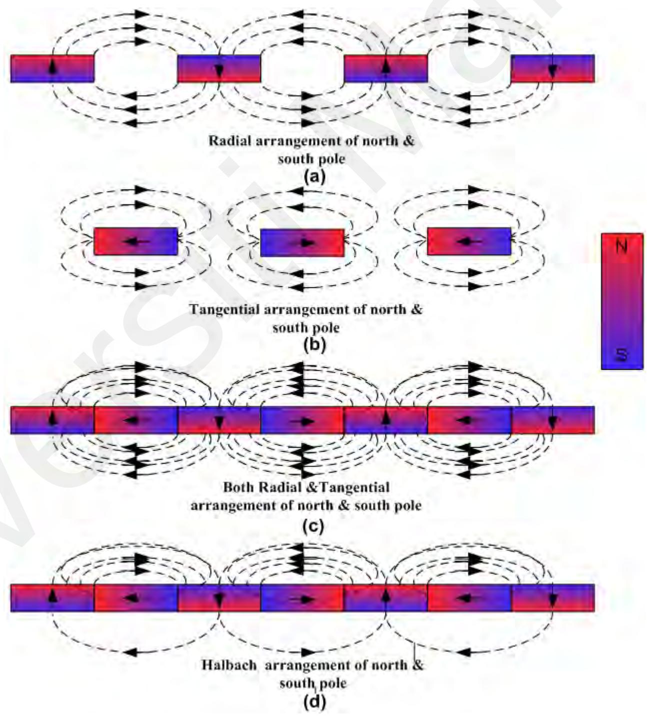

Figure 2.9: Conventional and Halbach array flux pattern

Most of the previous works on AFPM utilizes conventional magnet array, with only a handful of studies looked into the use of Halbach array(Zhu & Howe, 2001) reviewed the alternative Halbach machine topologies, where author described radial- and axial-field, slotted and slotless, rotary and linear (tubular and planar), and spherical Halbach magnetised brushless machines with different magnet like sintered rare earth magnet and NdFeB ring magnet, as well as their application.. Later, (Lee et al., 2004) introduced a design method of linear motor with segmented Halbach magnet array and investigated the difference in its performance with conventional Halbach array. Authors observed a certain extent of deviation in magnetic field in the strong side of the segmented Halbach array from the ideal case and reported that this deviation narrows down with increase in number of segmentations. For disc coreless permanent magnet synchronous motor, 90^0 Halbach array is applied in (QI et al., 2006), while author analyzed nine different PMs combination by FEM method since PMs thickness is the function of magnetic flux density in the air-gap. Author found that, the variation of the thickness of the tangential and radial magnetization PMs ensure a pure sine-wave of magnetic flux in the air-gap. In (Fei et al., 2010), the authors design, fabricated and analysed the performance of a prototype coreless AFPM generator with Halbach array arrangement, where author found a high magnetic flux in the air-gap using Halbach array. Design and analysis of an enclosed-rotor Halbach-array permanent-magnet brushless dc motors for spacecraft applications was presented in (Praveen et al., 2012). The authors found that the uniform air-gap flux density along the radius of the machine avoided circulating currents in stator conductors and thereby resulted in reduced torque ripples. (Winter et al., 2013) proposed three different method of Joule losses in a winding and Halbach magnets arrays for air cored axial flux motors while finally a full-scale prototype in wheel hub motor was manufactured based on the results of the three methods. The design of low speed direct drive axial flux permanent magnet generator with coreless stator and rotor for wind turbine power is discussed in (Chung & You, 2014), wherein Halbach array was implemented for strengthen the air-gap magnetic flux density. More recently, in (Ubani et al., 2016)a comparison between conventional AFPM with Halbach AFPM machine had been made by using FEA while three angle magnetization Halbach directions is applied for getting a high magnetic flux density in the air-gap which leads to a high torque. The author found that torque density is nearly doubled and tripled as in the case of the Halbach AFPM machine with Halbach-60º and Halbach-45º and the mass is halved. From Above literatures it can be concluded that Halbach magnet arrays are suitable only for limited types of machine, especially for axial flux machine where rotor one side magnetic field is not required.

2.5 Review Summary

From the literature reviewer, it was found that previous works on coreless AFPM machine focus mainly on the elimination of stator core (i.e. stator coreless) with rotor still having its back iron. The rotor back iron has two main functions: firstly it serves as a mechanical support structure on which the magnets can be firmly attached; secondly, the back iron provides a low reluctance path for the magnetic field which allows magnetic flux to travel across the air-gap instead of appearing as leakage flux on the outer-side of the rotor. To achieve better power density a light weight machine is always desirable; hence, non-ferromagnetic light materials like epoxy may be considered for rotor construction. However, simply removing the rotor back iron to form coreless or ironless rotor will increase the leakage flux and weakens the flux air gap flux density. This in turns reduces the performance of the machine. The use of Halbach magnet array, which is known to provide a single-sided magnetic field, seems to be a potential solution for this issue. While some studies have been done on the application of Halbach array on the rotor like, Halbach magnet array has been employed in axial-flux permanent magnet machines in different configuration and arrangements ranging from enclosed-rotor permanent-magnet brushless dc motors to linear motor with segmented magnet array. In addition, several researchers addressed the effect of factors like magnetization angle on the performance of Halbach array PM machines. However, application of Halbach magnet array in multi-stage topology in combination with

Universiti Malaya

conventional magnet array has not yet been reported in literature. Compared to single-stage AFPM machines, there is less studies done on multi-stage AFPM machines. The existing literatures usually obtain multi-stage AFPM machines by directly cascading multiple single-stage AFPM machine. However, the multi-stator multi-rotor structure of a multi-stage AFPM machine opens new possibility for innovative structure. Extending the concept of epoxy rotor with Halbach array from single-stage AFPM machine, it is interesting to see if a reasonably good multi-stage coreless AFPM generator can be obtained without using any iron structure in the stator and the rotor. A interesting feature is the presence of inner rotors and outer rotors in multi-stage AFPM generator. The outer rotors, which have the same requirement as single-stage AFPM generator, will need to use Halbach array to cancel the outer magnetic field, but the inner rotors can be constructed using conventional magnet array since they do not need to have single-sided magnetic field. The result is a multi-stage coreless AFPM generator with hybrid rotor structure that utilizes both Halbach and conventional magnet arrays. The performance of such machine needs to be evaluated and compared with direct cascade multi-stage AFPM machines.

Universiti Malaya

CHAPTER 3: RESEARCH METHODOLOGY

3.1 Introduction

The methodology for the project is explained in this chapter, where Figure 3.1 shows the overall flow of work done in this project.

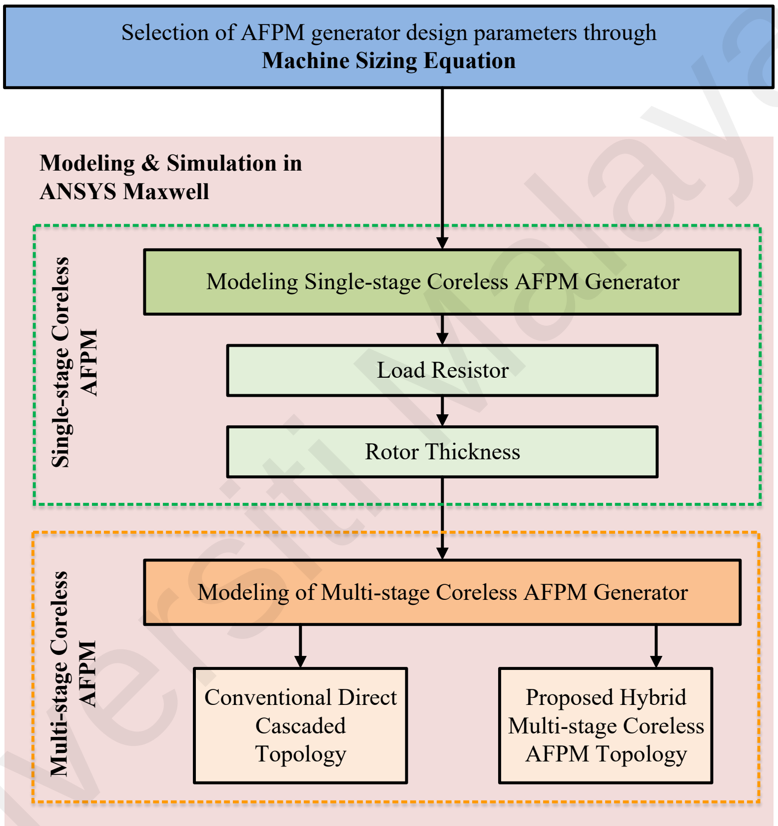

Figure 3.1: Work flow chart for the whole project

As seen from the flow chart, the project starts with the selection of AFPM Generator parameters using Machine Sizing Equations. Subsequently, the modelling and simulation of the generators are done using ANSYS® Maxwell, which can be divided into two stages. The first stage of the study involves the investigation of single-stage coreless AFPM generator with four different rotor structures using different combinations of magnet arrays and rotor materials. Using the findings on the first stage of the study, multi-stage coreless AFPM generators are modelled and simulated. A fully

Universiti Malaya

coreless multi-stage AFPM generator is proposed using hybrid rotor structure in the second phase of the project. The proposed generator is compared with multi-stage AFPM generator obtained by directly cascading single-stage AFPM generators from the first part of the project. Details on each step in work flow are given in subsequent parts of this chapter.

3.2 Selection of AFPM Generator Parameters through Sizing Equation

For analytical design, some initial design assumptions are necessary to establish the whole model based on sizing equations. The parameters for initial assumptions are phase number (m), output power (P_o), speed (ω_s), magnetic loading (B_g), electrical loading (A_m), ratio of inner and outer diameter (λ), power factor ($cos\varphi$), efficiency (η), the values being given in Table 4.1 in chapter 4. For machine design the first important and one of the main parameters is outer diameter (D_{out}).

3.2.1 Machine Sizing Equation

Based on sizing equation, the D_{out} can be determined as (Huang et al., 1999; Mahmoudi et al., 2013):

$$D_{out} = \left(\frac{P0}{\frac{\pi}{2} K_{size} B_g A_m \eta \frac{f}{p} (1-\lambda^2)(\frac{1+\lambda}{2})}\right)^{\frac{1}{3}} \tag{1}$$

where $K_{size}=k_e.ki.k_P$ For sinusoidal waveform the values of k_e, k_i, k_p are briefly explained in (Huang et al., 1999; Mahmoudi et al., 2013) where maximum parameter's value required in equation (1) comes from the very initial assumption. The important parameter air gap magnetic flux density B_g is normally dependent on the magnet geometry as well as magnet grade.

Universiti Malaya

The ratio of inner and outer diameter (λ) is considered as another important parameter for AFPM machine design, because it plays an important role in maximizing the output power. From previous research, different optimized values of λ were chosen for different AFPM design, out of which $1/\sqrt{3}$ and $1/\sqrt{2.5}$ are the common for the most of the configurations (Chan & Lai, 2007; Daghigh et al., 2017; Upadhyay & Rajagopal, 2006). Usually, for iron core rotor, the iron structure itself deals with the magnetic field as magnetic field has a strong contribution to output torque as well as power. On the other hand, for pure coreless rotor and stator, the magnetic field is not active in the body of the rotor. Thus, only the magnet is responsible for building up the magnetic field. In the present study, as the rotor is coreless, so λ is the ratio of inner to outer diameter of the magnet, and the length of the magnet is dependent on λ also.

The primary assumption, rotating speed ω_s helps to determine the pole number and from pole number the coil number can be easily determine by (2) and (3).

$$\omega_S = \frac{120f}{p} \tag{2}$$

$$Q = \frac{3}{4} th \times p \tag{3}$$

where f is the frequency, p is the pole number and Q is the number of coils. The electrical loading (A_m) was a primary assumption and also can feed to the sizing equation by determining with equation (4) (Huang et al., 1999).

$$A_m = 4mN_{cph} I_{ph} \big/ \pi D_{out} (1+\lambda) \tag{4}$$

where N_{cph} is the number of conductors per phase I_{ph} is the current per phase. N_{cph} comes from the number of turns per coil N_c. From equation (5) N_c can be determined as

Universiti Malaya

$$N_c = \frac{\pi \alpha_w D_{out} (1+\lambda) A_m}{4QI_{ph}} \tag{5}$$

where a_w is the number of parallel current paths.

3.2.2 Rotor Design

For an AFPM generator, the rotor part is equipped with the magnets. So, the components of rotor are the magnets and the rotor back yoke. For a fixed diameter of rotor back yoke the magnets geometry is very important to fit in. Thus, the magnet geometry should be calculated according to the diameter of the rotor back yoke. Apart from that, based on magnet arrangement there are two topologies (conventional and Halbach magnet arrangements) are discussed here for comparing of the generators.

3.2.2.1 Magnet geometry

For air-gap magnetic flux density B_g and PM axial height h_{pm} has a strong contribution as shown in equation (6)

$$h_{pm} = \frac{\mu_m B_g (L_{sc} + 2g)}{2(0.9B_r - \frac{B_g}{K_{pm}})} \tag{6}$$

where μ_m is the magnet permeability, B_r is PM residual flux density, g is air-gap length and K_{pm} is PM leakage flux factor. As the machine is pure coreless, the inner and outer diameter is the magnet outer and inner diameter. With the magnets being arranged in a circular way, the distance between the outer and inner diameter is the magnet length (l_{pm}) refer to equation (9). Figure 3.2 shows the magnet geometry. For magnet width (w_{pm}), the equation (7) and (8) can be used for calculation of magnet widths.

Universiti Malaya

$$w_{pmo} = \frac{2\pi r_o - (n_M \alpha_p)}{n_M} \tag{7}$$

$$w_{pmi} = \frac{2\pi r_i - (n_M \alpha_p)}{n_M} \tag{8}$$

$$l_{pm} = w_{pmo} - w_{pmi} \tag{9}$$

where n_M is the total number of magnets. The magnet is trapezoidal as a result there are two widths for inner and outer diameter of the magnet.

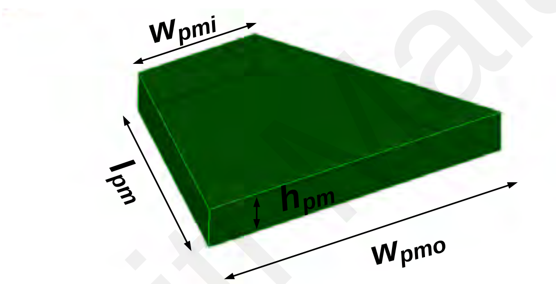

Figure 3.2: Geometry of the magnet

(a) **Conventional magnets arrangements in rotor:**

For single-stage AFPM machine, the magnets on the two-disc rotors are separated by an axial gap within which the stator coils will be located. The magnetic field within the gap is detrimental to the overall machine performance. Normally iron core rotors enhance the magnetic field and as a result, higher air-gap magnetic flux density leads to higher power. Furthermore, the iron rotor confines the flux, avoiding flux leakage towards the external sides of the rotors. In the case of a conventional magnets array without iron rotor, the magnetic field is active for both side of the array and the use of epoxy martial for the rotors leaves one side of the array unused. That is why for conventional array iron core rotors are preferable for an AFPM machine. Figure 3.3 shows the poles and magnet arrangements for conventional array.

Apart from that, in conventionalarray, two magnets create one pole pair. Figure 3.4 shows the pole pair wavelength (l_a) of conventional arrays. The definition of l_a has been discussed briefly in section 3.2.2.1(b). Here magnet width to pole pitch ratio (a_P) defines the gap between the magnets. For conventional array an optimum gap a_P between the magnets is very necessary to get a high air-gap magnetic flux.

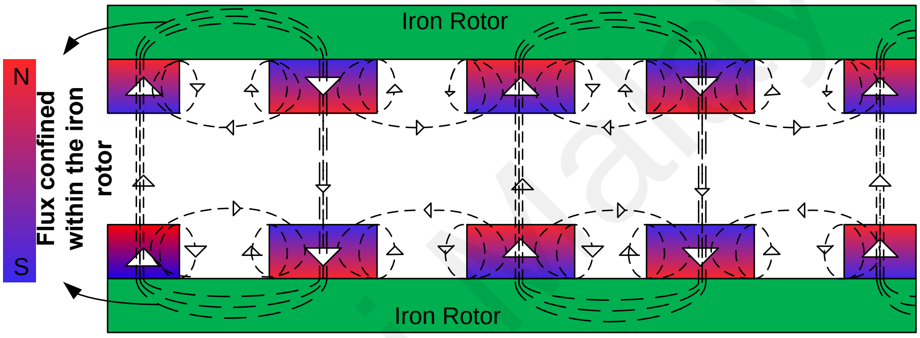

Figure 3.3: Pole positions with an opposite arrangement (N-S type) and the associated flux paths for conventional array in single-stage coreless AFPM

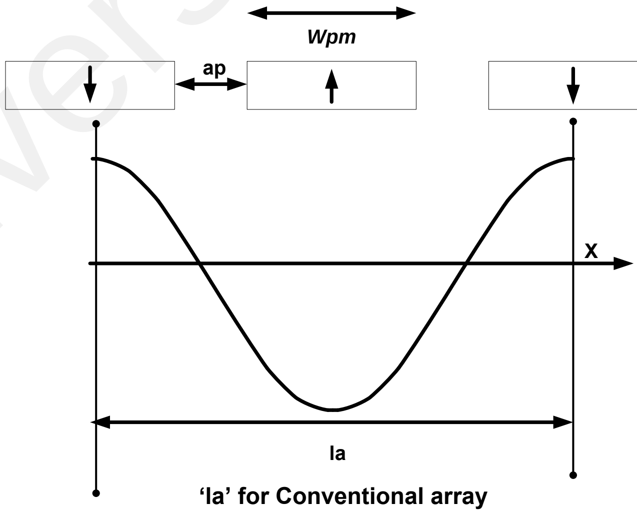

Figure 3.4: Wavelength (l_a) for conventional array

Universiti Malaya

(b) **Halbach magnets arrangements in rotor:**

Halbach Array is a combination of two conventional (radial and tangential) arrangement of north and south pole. The arrangement of north and south pole in Halbach array helps to strengthen the field in one side of the array while canceling out the field on the other side (Zhu et al., 2013). Figure 3.5 shows the flux patterns of Halbach array in single-stage coreless AFPM generators.

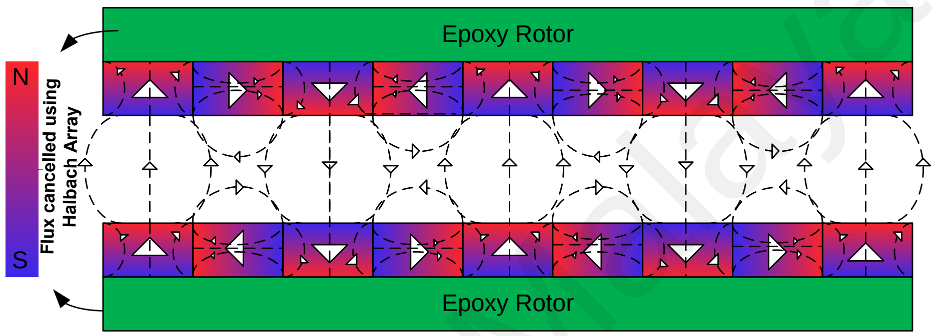

Figure 3.5: Pole positions with an opposite arrangement (N-S type) and the associated flux paths for Halbach array in single-stage coreless AFPM

For ironless rotor structure, Halbach array can be useful by cancelling out the fluxes on the back of the rotor and strengthen up the field to the active side of the array, thus help to obtain high magnetic flux density in the air gap that leads to the high power density (Gieras et al., 2008). The epoxy materials used in stator and rotor are temperature and pressure resistant. Apart from that, the pole pair formation due to magnets is different from one another. In conventional array, two magnets create one pole, whereas in Halbach array four magnets create one pole. Figure 3.6 shows the pole pair wavelength (l_a) of Halbach arrays. Here magnet width to pole pitch ratio (a_P) defines the gap between the magnets. For Halbach array to strengthen the field in one side of the array, the gap (a_P) should be as less as possible.

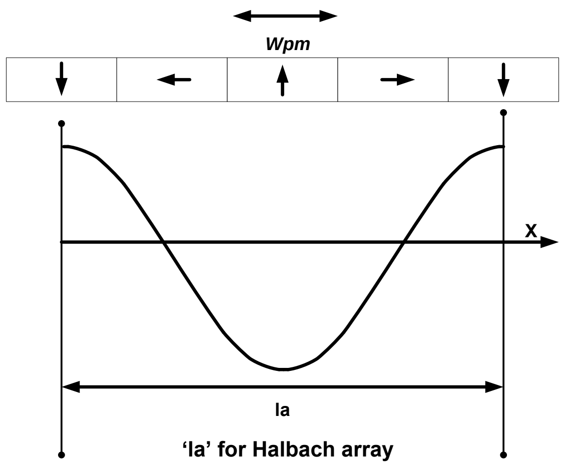

Figure 3.6: Wavelength (l_a) for Halbach array

3.2.3 Flux Density in the Air-Gap

The main difference between the Halbach and conventional array is on the magnetic flux density and distribution. Geometry and other parameters can be kept the same for fair comparison except for the magnet size. Since the two topologies have different characteristics, the size of the magnet cannot be the same for a fixed rotor diameter. The number of magnets used for Halbach configuration is double that of the conventional array. Nevertheless, for fair comparison, the same total magnet volume should be maintained. To achieve this, the axial height of the magnets is adjusted while keeping the radial length of the magnet constant. Though the wavelengths are same for the both conventional and Halbach, they have different effect for magnet width to pole pitch ratio a_P. For conventional rotor, optimal a_P is required for less torque ripple with maximum average torque (Kim et al., 2007). On the other hand, Halbach rotor needs to minimize the gap between magnets (a_P=1) to ensure effective cancelling of magnetic field on one side and the strengthening of flux on the other side. Thus, there are two different equations for calculating B_g. The equations of the air gap magnetic flux density of Halbach array and conventional array can be written as (10) and (14).

$$Bg(h) = Br[1 - \exp(-\beta h_{pm})]\frac{\sin(\pi / n_{Ml})}{\pi / n_{Ml}} \qquad (10)$$

where β is the $2\pi/l_a$ and l_a is the spatial period (wavelength) of the array, n_{Ml} is the number of magnets per wavelength. For $l_a$the value differs for the two different topologies of Halbach array and conventional array. For Halbach array, four magnets create one full wavelength or one pole pair as there is no gap between the magnets, refer to (11) (Gieras et al., 2008).

$$l_a = 4w_{pm} \qquad (11)$$

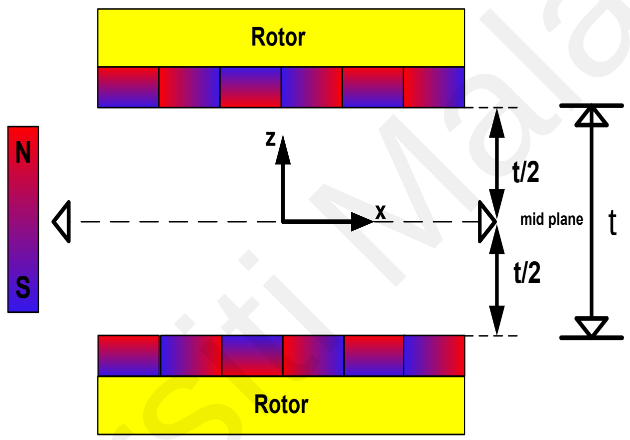

Figure 3.7: Plane region for air-gap magnetic flux density

From equation (10) the peak value of magnetic flux density at the active surface of Halbach array can be calculated. As seen in Figure 3.7the tangential and normal component of the magnetic flux in the space between two discs are given by (Gieras et al., 2008)

$$B_x(x,z) = B_g \frac{1}{\beta}\cos(\beta x)\frac{2\sinh(Bz)}{\exp(\beta t / 2)} \qquad (12)$$

$$B_z(x,z) = B_g \sin(\beta x)\frac{2\cosh(Bz)}{\exp(\beta t / 2)} \qquad (13)$$

where B_x is the tangential component (along the x-axis), B_z is the normal component (along z-axis).

For the proposed design, the normal component is higher than the tangential component. At a glance, the value of B_z is minimum in the middle of the two rotor discs and maximum at the surface of the magnets. For conventional array the equation (Virtič et al., 2016) is given by

$$B_g(c) = \frac{1}{\mu_0} \int_S r B_x B_z dS \tag{14}$$

where μ_0 is the permeability of free space, r is the radius of the rotor; S is the integration surface of the mid plane of the air-gap. B_x and B_z depend on the optimized geometry of the machine parameter, like a_P.

3.2.4 Stator Design

Being coreless, only the stator coil needs to be present ideally. However, in practice, a rigid and strong structure is needed to hold the coils in place and restrain their movements during operation. For this, epoxy hardener is used. Therefore, there are two parts are considered for the stator design. One is coil and another part is the epoxy hardener frame. In order to design a stator for single-stage coreless AFPM generator the coil geometry and the thickness of the epoxy hardener frame are theoretically analysing and discussed in this section.

3.2.4.1 Coil geometry

The coreless non-overlapping concentrated windings have been used for the present design. For higher efficiency and low cost, this winding is the better choice as non-overlapping concentrated coil needs less volume of copper results in reduction of copper losses and finally increase in generator efficiency. In this design single layer trapezoidal coil shape is chosen for shortening the end winding length (l_e) as compared to active coil length (l_{act}) of the coil that helps to maximize the coil flux linkage. A shorter l_e reduce the resistive losses in the inactive part of the coil. The calculation of l_e and w_c have been done with equations (17) and (18) respectively (Rossouw, 2009). Figure 3.8shows the schematic of the coil geometry and its position with respect to magnet. As the stator is coreless, the saturation of magnetic flux in the stator core can be totally neglected. On the other hand, only the stator coil axial height (L_{sc}) and coil cross section area (S_w) are considered because the coil height has an impact on the geometry of the axial height of the machine via the air-gap length from magnet associated rotor disk to another side of rotor disk. An optimized L_{sc} is required for a better output power. A large L_{sc} increase the total air-gap length as well as the active area length of the magnetic flux density and finally will decrease the magnetic flux density in the air-gap.On the other hand, very short axial length will force to increase the S_w, in a result large width of coil w_c. But for a fixed diameter the high w_c creates difficulty to fit all the coils in the limited circular space. The L_{sc} and S_w can be referred to equations (15) and (16) as follows:

$$S_W = \frac{2I_{ph}N_c}{K_f a_w J_a} \tag{15}$$

$$L_{sc} = \frac{2S_W Q}{k_s \pi D_{in}} \tag{16}$$

where K_f is the fill factor, J_a is the current density, and k_s is the space utilization factor. For coil wounding K_f is an important factor as it signifies the cross section of the coil S_w. As a rule of thumb, the value of K_f for manually constructed winding with circular cross section is around 0.55 to 0.78 (Latoufis et al., 2012) The factor k_s is related to the mechanical strength of the stator structure. Coreless structure should be mechanically strong enough to hold the coils and against the attraction of magnet.

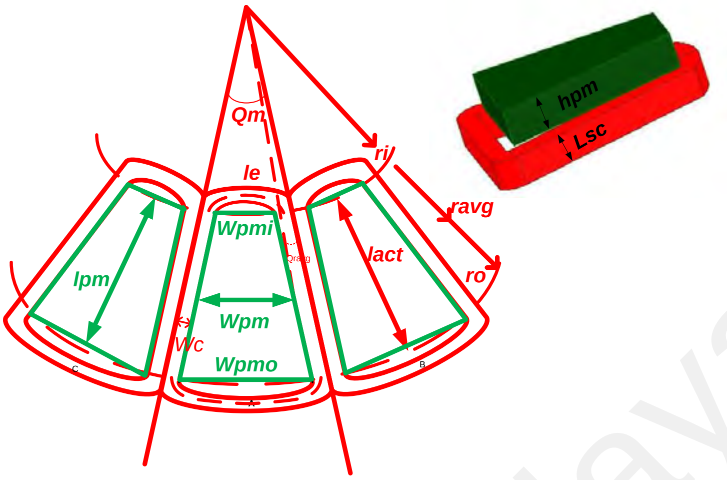

Figure 3.8: Magnet and coil geometry

Winding factor (K_w) is another important parameter for the coil design as well as the total torque and the power. A value between $0.9 \leq K_w \leq 1$ is optimized for choosing the winding factor (Kamper et al., 2008).

3.2.4.2 Epoxy frame thickness

The coreless stator is advantageous for the machine as core loses can be eliminated from coreless stator. On the other hand, without core the stator becomes very frail. To ensure sufficient mechanical strength of stator disc, it is necessary to consider the required thickness and space for the epoxy resin in the internal radius of the machine. The equation of minimum value of winding axial length L_{sc} for single layer nonoverlapping winding coils, with consideration of space utilization factor ks, can be found in equation (16).

Universiti Malaya

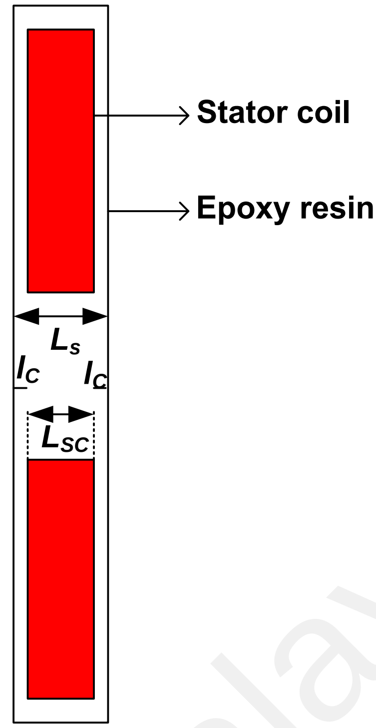

Figure 3.9: Whole stator thickness including coil and epoxy resin

The AFPM machine has two components of the magnetic field in the air-gap: one is normal component working axially and the another is the tangential component which actually represents the leakage flux. So, there is a interaction betwen the tangential component of the magnetic filed and the coil currents, which causes an axial magnetic force on each coil. As a results, stator feels an unbalanced force which effect the mechanical strength of the epoxy resin stator disk. Regarding this axial force and considering the conditions of coils winding, the axial length of the resin stator disc (L_s) is assumed to begreater than the axial length of coils, which is expressed in equation (17) and illustrated in Figure 3.9.

$$L_S=L_{sc}+2l_c \quad (17)$$

where l_c is the axial increment on each side of the stator resin disc, which is chosen to be 0.5 mm in this study.

Universiti Malaya

3.2.5 Induced Voltage

The induced voltage calculation is dependent on coil geometry and placement as the nonoverlaping concentrated windings have some parameters directly affect the voltage. The RMS value of sinusoidal phase voltage of non overlaping winding E_v can be determined by (18) (Kamper et al., 2008).

$$E_v = \frac{q_p}{a_w}\frac{2\sqrt{2}}{p} w_s B_{gp} N_c r_{avg} l_{act} k_p k_d \tag{18}$$

where q_p is the number of stator coils per phase, B_{gp} is the peak air-gap flux density, r_{avg} is the average radious of the stator winding, l_{act} is the active length of the coil, k_p is the pitch factor of the non overlaping winding and k_d is the distribution factor. The pitch factor k_P and the distribution factor k_d can be calculated by equation (19) & (20) (Rossouw, 2009). In Fig. 4, r_{avg} and θ_m, θ_{avg} are shown.

$$k_p = \frac{\sin(\theta_m \frac{[1-\kappa]}{2} \sin(\frac{\kappa\theta_m}{2})}{\frac{\kappa\theta_m}{2}} \tag{19}$$

where $\theta_m = \frac{\pi p}{Q}$ and $\kappa = \frac{\theta_{r_{avg}}}{\theta_m}$

$$k_d = \frac{\sin(n\frac{[\theta_m - \pi]}{2})}{n\sin(\frac{[\theta_m - \pi]}{2})} \tag{20}$$

Universiti Malaya

3.2.6 Magnetic Pull on Rotor Discs

Due to the constraction of single-stage AFPM generator, the magnets on the two rotors facing each other will have opposite polarity. For rotors with iron structure, magnetic force will exist between opposing magnets, as well as between magnet on one rotor with the iron structure of the opposite rotor. For coreless rotor however, only the magnet to magnet attraction will be present. The attraction force due to two magnets placing in a distance of g apart, with a magnet surface area of S_{PM}, a magnet thickness of t_M and an air-gap magnetic flux density B_g can be expressed as follows:

$$F = \frac{2.B_g{}^2 t_M{}^2 S_{PM}}{\mu_0 g^2} \tag{21}$$

3.3 Modeling AFPM Generator in ANSYS® Maxwell

The ANSYS® Maxwell software is used for the modelling and simulation of the single-stage and multi-stage coreless AFPM generators. The total machine simulation is carried out by two different simulation process, one is magneto static solution and another one is transient solution. The flow chart of ANSYS® Maxwell modelling is given in Figure 3.10.

Universiti Malaya

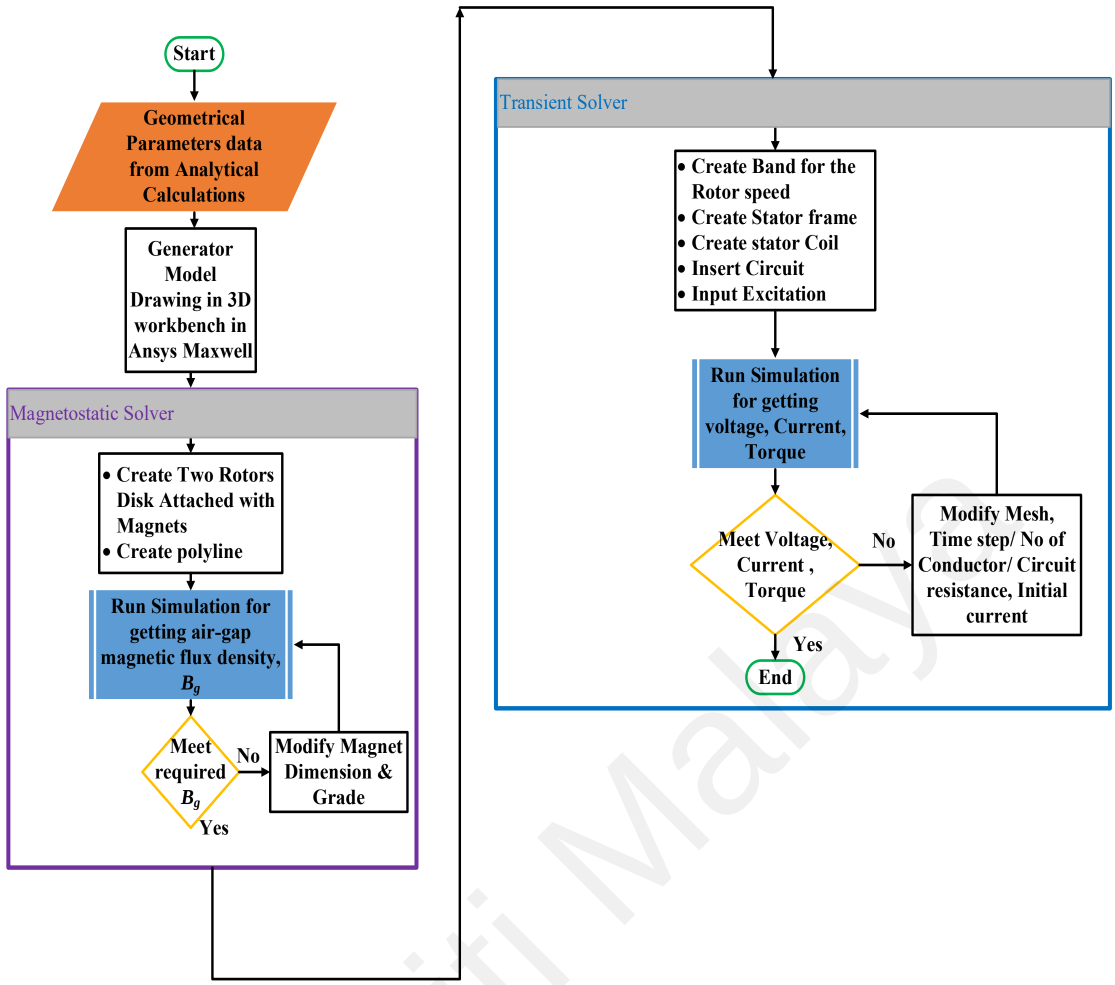

Figure 3.10: Flow chart of AFPM generator modeling in ANSYS® Maxwell

At first the AFPM generator is modelled in a 3D workbench in ANSYS® Maxwell with the help of geometrical parameters getting from analytical calculations. After geometry creation of the AFPM generator, the important poly line creation, band creation, excitation, speed modelling has to use for setting up the simulation. In order to reduce simulation time, the Magnetostatic solver is first used to quickly evaluate the flux density of the generator, which will affect the voltage, current, hence power of the generator. Based on the flux density, magnet dimension needs to be modified until satisfactory flux level is obtained. Subsequently, the Transient solver is used to obtain the generator's voltage, current, torque and power performance.

3.3.1 Magnetostatic Simulation

All kind of magnetic solutions have been done on this part. For machine design air-gap magnetic flux density is an important parameter for design. Magneto static solution solves for the air-gap magnetic flux density. B_g is tested by imagining a mid-plane between the two rotors called polyline. In order to do that, the rotors associated with magnets need to be set properly from the drawing, while magnet polarity is given to the magnet with the help of face creation. After completing the magneto static simulation, the magnetic flux density in the mid air-gap (B_g) between the two rotors is found sinusoidal, throughout the polyline area. The peak value from the sine-wave is chosen for the magnetic flux density (B_g) acting on the mid air-gap of the two rotors. However, for getting the desired B_g the mesh setting needs to be fine-tuned, before and during the simulation-running while 0.7 T is the targeted B_g for this project. In addition, a proper magnet grade parameters and dimension can be modified for a higher magnetic flux density. The snap shot for Magnetostatic solver from the ANSYS® Maxwell is given underneath in Figure 3.11 for a better understanding.

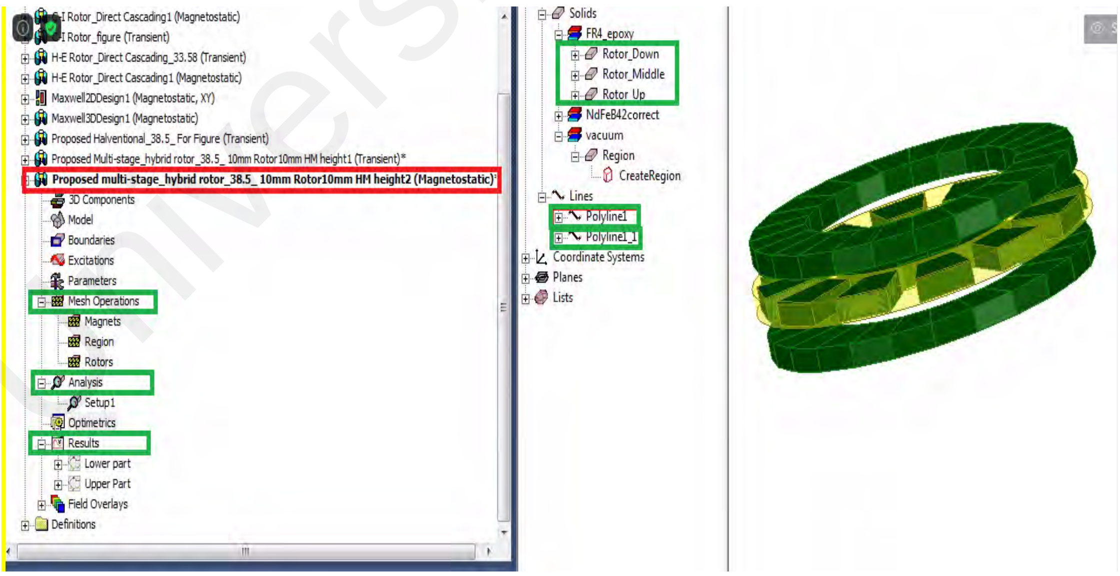

Figure 3.11: AFPM generator modeling in ANSYS® Maxwell software in magnetostatic solver

Universiti Malaya

3.3.2 Transient Simulation

All kind of final output results like voltage, current, flux linkage to the coil, torque, torque ripple etc considering the rotational motion of the generator are simulated in this part. For transient solver, at first a constant speed is given to the rotor by introducing a model called band. The band creation is nothing but setting the speed as one of the inputs, of generator. Apart from that the stator frame and coil is modelled with their proper excitation for complete the geometry set up. However, the three-phase full load circuit is needed to set before going to analyze the simulation. Nevertheless, for a proper /desired output from the simulation the mesh setting, time step, number of conductors, resistor of the circuit and initial current need to be adjusted during the simulation-running. The output results (voltage, current, torque) are automatically created in the results options and only for torque ripple the parameters value need to be set in the results settings. The snap shot for Transient solver from the ANSYS® Maxwell is given underneath in Figure 3.12 for a better understanding.

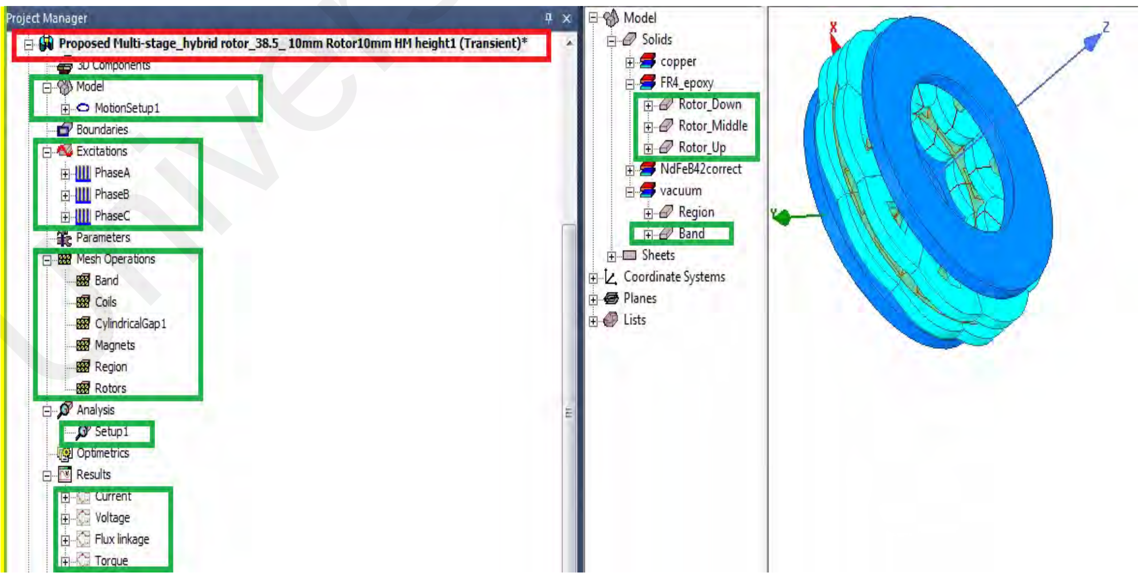

Figure 3.12: AFPM generator modeling in ANSYS® Maxwell Software in Transient solver

Universiti Malaya

3.4 Modeling of Single-stage Coreless AFPM Generator

Single-stage coreless AFPM machine has a single internal coreless stator between two external PM rotor discs. The stator coils are single layer concentrated windings of trapezoidal geometry, embedded in an epoxy, and covered with composite material hardener to ensure enough mechanical strength for the whole stator structure. The rotor structure is formed by trapezoidal shape magnets, rotor support structure, and shaft. The two discs shaped rotor carry the axially magnetized NdFeB magnets mounted axially on the inner surfaces of the two rotor discs. NS type flux direction is travelled axially from one rotor disc to another rotor disc via the coreless stator. The air gap between the rotor and stator are kept at 0.5 mm on both sides. Figure 3.13 shows the work flow chart for the design and comparison for single-stage coreless AFPM generator.

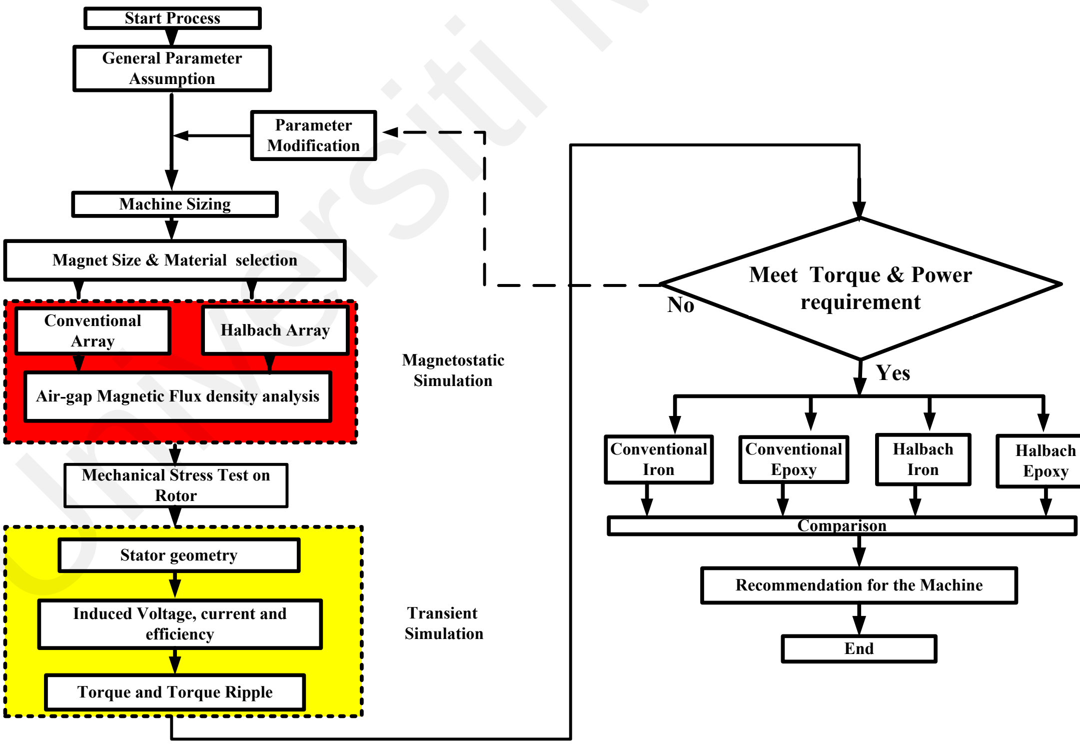

Figure 3.13: Work flow chart for the design and comparison for single-stage coreless AFPM generator

Figure 3.14 represents the whole model for single-stage AFPM machine and the associated flux path.

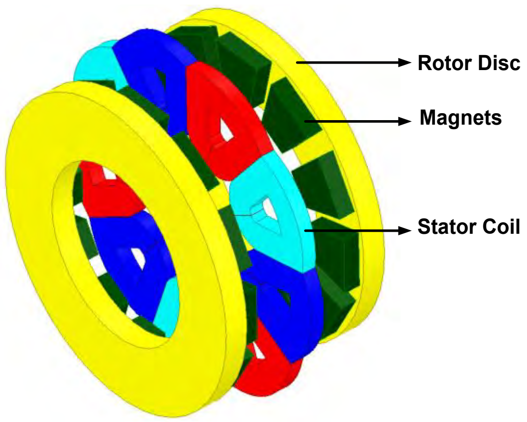

(a)

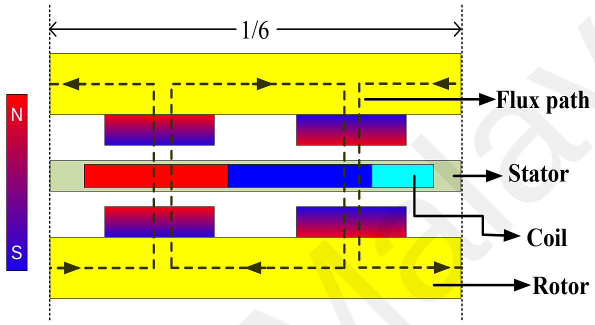

(b)

Figure 3.14: Design of 3-phase conventional single-stage coreless AFPM generator(a) complete model for conventional (b) flux path (NS type) in 1/6 of the design

In the present research, four different single-stage coreless AFPM generators have been designed with the same parameters for comparison. The two different magnet arrangements (Conventional and Halbach), are combined with two different materials (iron and epoxy) of the rotor, to give the following four topologies:

i) Conventional magnet array with iron rotor (C-I Rotor)

ii) Conventional magnet array with epoxy rotor (C-E Rotor)

iii) Halbach magnet array with iron rotor (H-I Rotor)

iv) Halbach magnet array with epoxy rotor (H-E Rotor)

The major difference among the four topologies lies in the arrangement of the magnets and disparity of materials for the rotor discs. The differences are shown clearly

Universiti Malaya

in Figure and Figure. The four topologies all have 12 poles, for a speed of 500 rpm at 50Hz. Though conventional and Halbach arrays have different magnet width due to magnet width to pole pitch ratio, their magnet thickness is different such that the total volume of magnets (hence, the magnet cost) is kept constant for all four topologies.

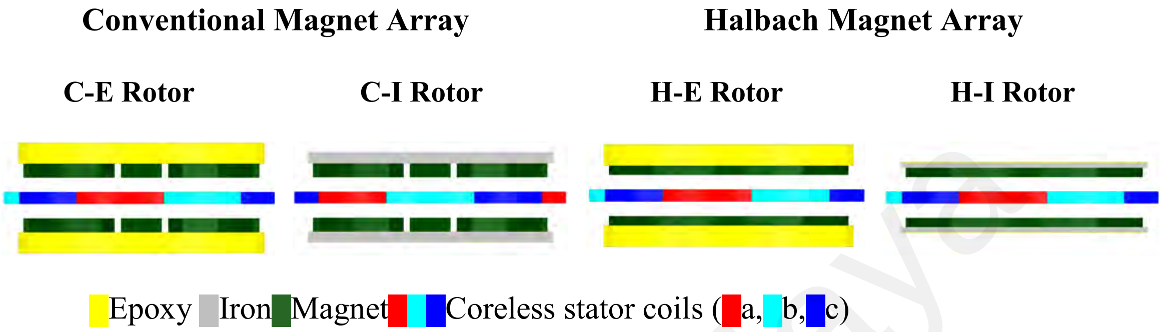

Figure3.15: Centre aligned side view of the four different generators for overall comparison

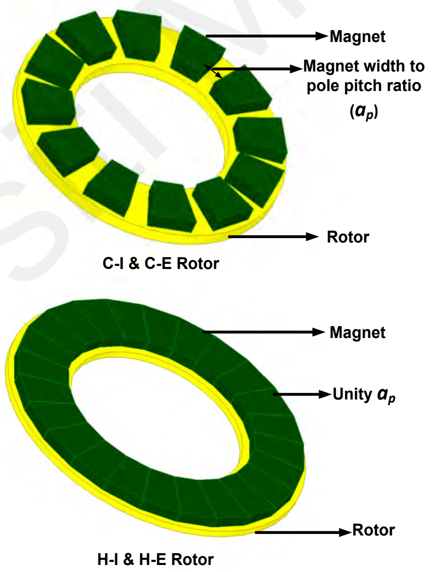

Figure3.16: Rotor with conventional (C-I Rotor and C-E Rotor) and Halbach (H-I Rotor and H-E Rotor) magnet arrays

3.4.1 Load Resistance

In order to make a fair comparison of the different rotors and the magnet arrangements the designs need to fix a same current loading for all the stator of different machine. As the geometry and the number of conductors of the stator coil for all the machines are same, a fixed current is used by choosing different loading. From the wire

Universiti Malaya

gauge conductor size, AWG-16 is used for this design which is chosen according to the coil geometry and conductor number. The maximum current carrying by AWG-16 is 3.7 A. Thus, 5.23A peak current or RMS 3.7A is fixed for all the stator electrical loading. To identify the different loading for different machines a test is conducted in Figure by fixing the current for all the four machines.

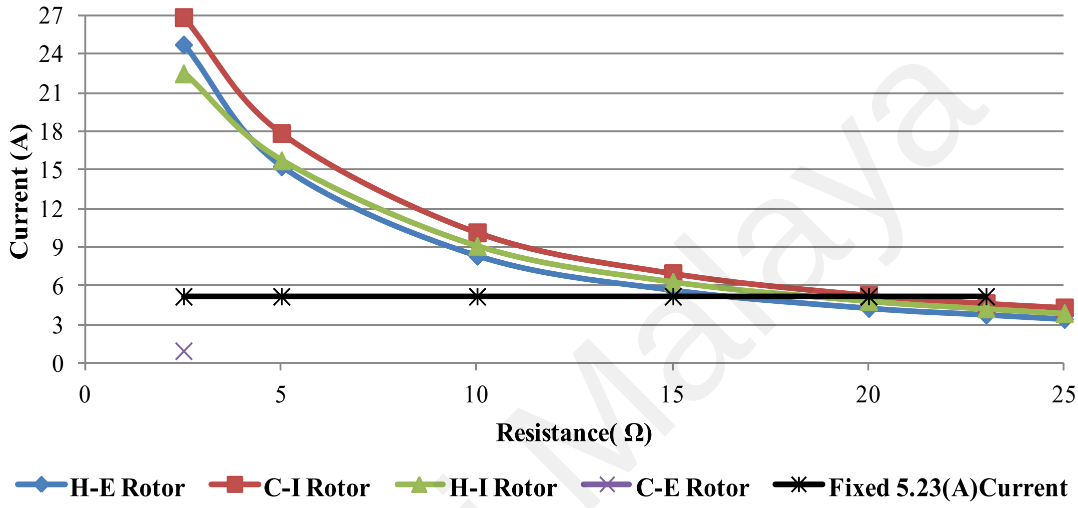

Figure 3.17: Current vs. different loading test

The test is conducted for the four machines in ANSYS® Maxwell software. Figure shows the zoom in image of the Figure.

Universiti Malaya

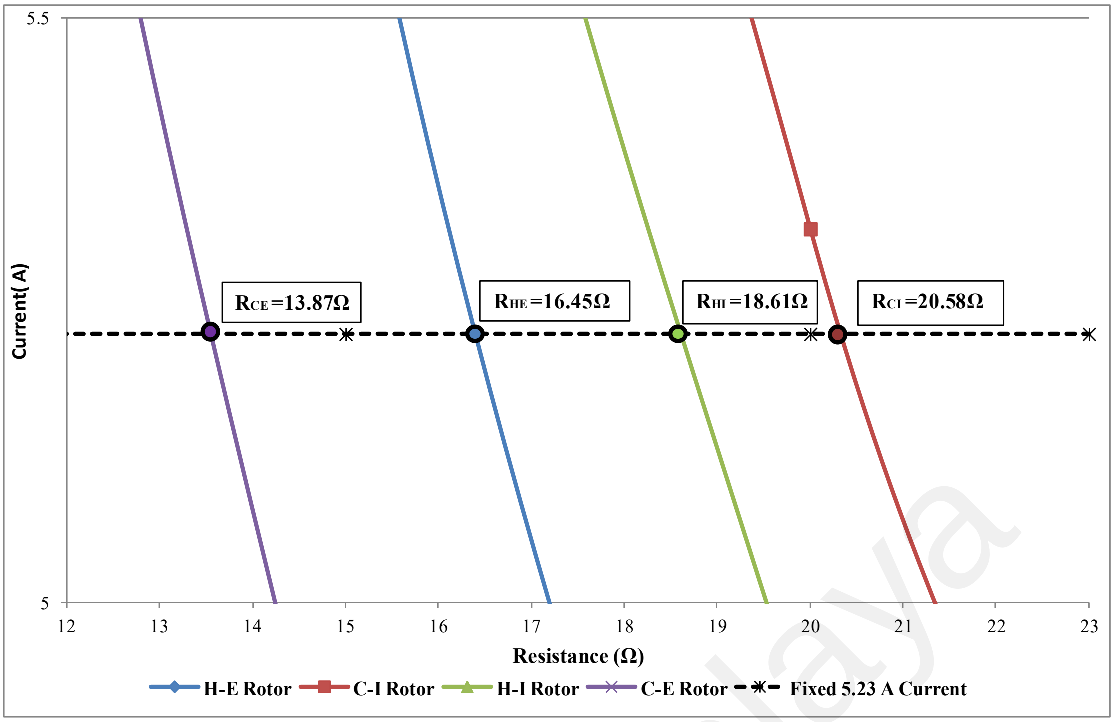

Figure 3.18: Current vs. Different loading test (zoom in image)

3.4.2 Rotor Thickness

The thickness of the rotor is a trade-off between cost and performance: excessive rotor thickness will cause unnecessary increase in cost and weight, while insufficient thickness can lead to flux saturation and leakage which degrades the machine's performance. Hence the selection of rotor thickness needs to be considered properly.

Here, flux density B_g, leakage flux and mechanical deflection of the rotor, have been analyzed and examined for the four topologies. In order to minimize cost and the size, the rotor should be as thin as possible but thick enough to ensure no significant leakage flux appear on the external surface of the rotor. For iron rotor, air-gap magnetic flux density depends on the rotor thickness, as thin rotor will result in flux saturation which reduces the flux density. Sufficient thickness is also important to give enough mechanical strength such that the magnetic attraction force between the two rotors will not cause significant mechanical deflection of the rotors. The electromagnetic and mechanical tests are analyzed using ANSYS® Maxwell and AutoCAD Mechanical design software, respectively. The whole selection of design parameters is presented in Figure.

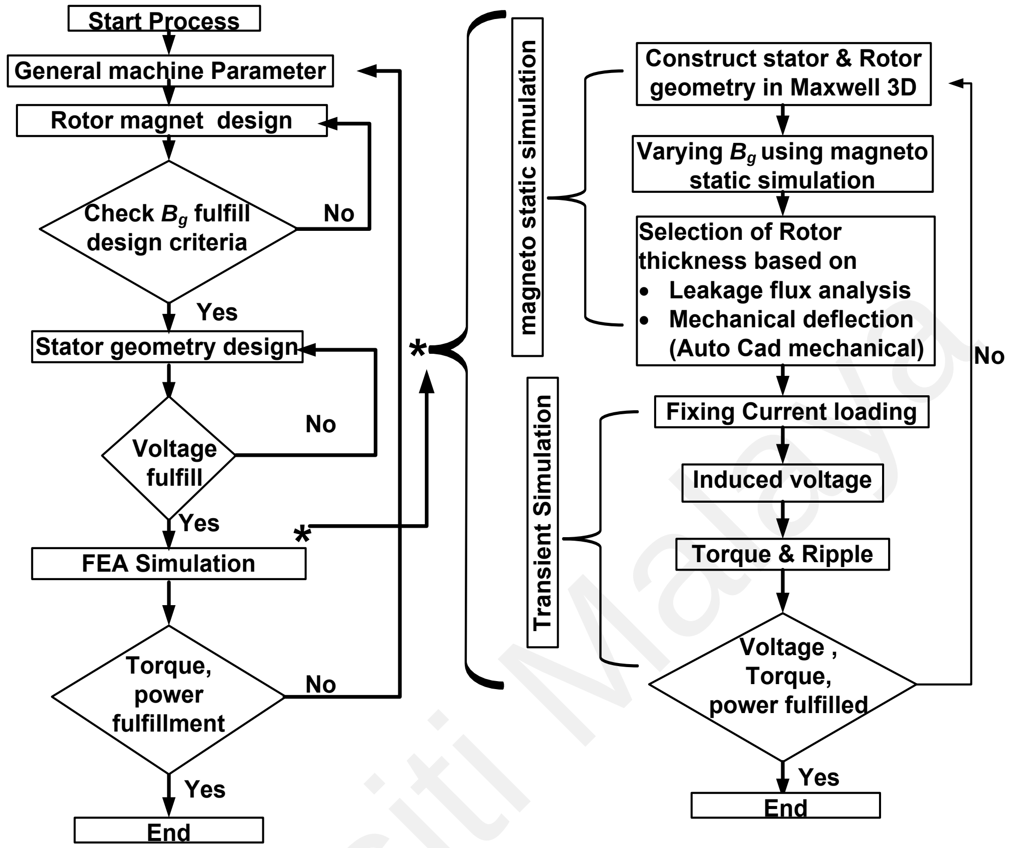

Figure 3.19: Flow chart for selections of design parameters in FEA

3.4.2.0 Air-gap Magnetic Flux Density (B_g)

The magnetic flux density (B_g) is a function of iron rotor thickness. As the relative permeability of the ferromagnetic material follows the B-H curve so the material should have a saturation point for magnetic flux. If the rotor back iron is too thin, the magnetic flux will be saturated causing leakage flux on the external side of the rotor, which reduces the B_g value. Figure shows that the air-gap magnetic flux (B_g) increases with the increase of rotor thickness up to a saturation point beyond which further increase in rotor thickness does not increase the flux. From the FEA analysis, it can be seen that saturation occurs earlier in Halbach array than that in conventional array. This indicates that Halbach rotor requires thinner rotor to maximize the air-gap flux. However, if the rotor thickness is allowed to increase further, conventional magnet array is able to give higher air-gap flux for the same magnet volume.

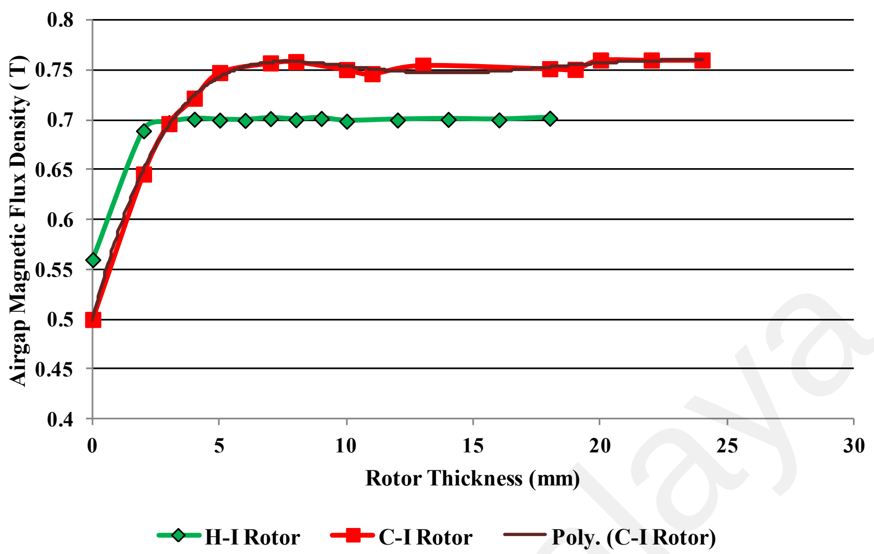

Figure 3.20: Ferromagnetic rotor thickness vs. air-gap magnetic flux density of conventional and Halbach array

3.4.2.1 Leakage Flux Analysis

Apart from B_g, the rotor back iron should also be thick enough to ensure no significant leakage flux. The leakage flux is tested on a distance of 0.01mm from the rotor upper surface of the four topologies. The test has been done in ANSYS® Maxwell magneto-static solution. A line is drawn at a distance of 0.01 mm from the rotor upper surface and simulated for all four topologies with various thicknesses. In Figure, leakage flux with rotor thickness variation is shown. Halbach rotor has lower leakage flux than the conventional rotor, due to flux cancellation effect. Halbach array requires much lower rotor thickness (around 2 mm) to reduce leakage flux to a negligible range, than conventional array (around 7 mm).

Universiti Malaya

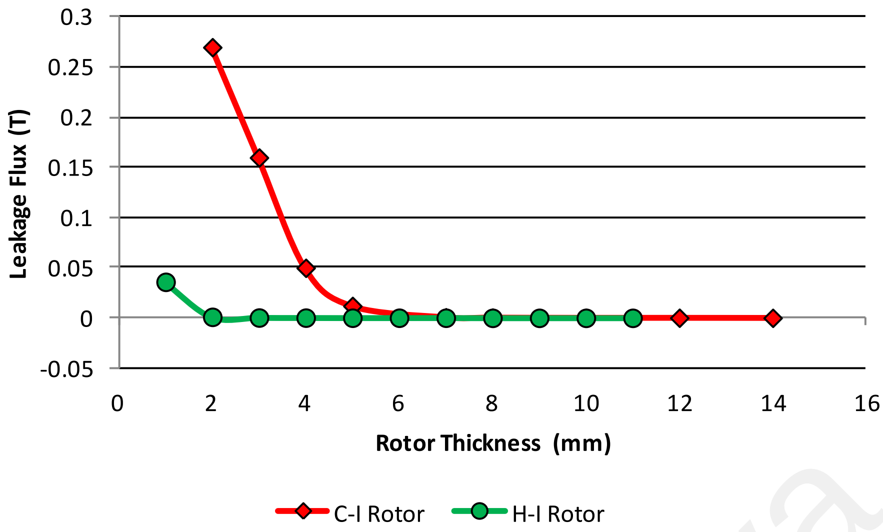

Figure 3.21: Iron rotor thickness vs. leakage flux of conventional and Halbach array

3.4.2.2 Mechanical Deflection

For the construction of the single-stage AFPM machine, the two opposite rotors attached with magnets are attracted to each other. Although attraction force works for both ferromagnetic and non-ferromagnetic rotor, for non-ferromagnetic rotor it is slightly less. The strong attraction force between the magnets imposes an opposite pulling force on the rotor that tends to bend the rotor structure leading to a collision between the rotor and stator or can reduce the air-gap distance between them; as a result, a non-uniform and unbalanced magnetic flux density will be formed in the air-gap. Hence, mechanical deflection is another important point of consideration to design optimum rotor thickness for the four topologies. Force calculation for the magnetic pull on rotor discs is done by using equation (21). To find an optimum thickness of the rotor, the force is applied to the various thickness of the rotor for both ferromagnetic and non-ferromagnetic material. Figure shows the deflection of the rotor from von Mises stress analysis for the four topologies, while Figure shows the von Mises test results from the AutoCAD Mechanical Design software.

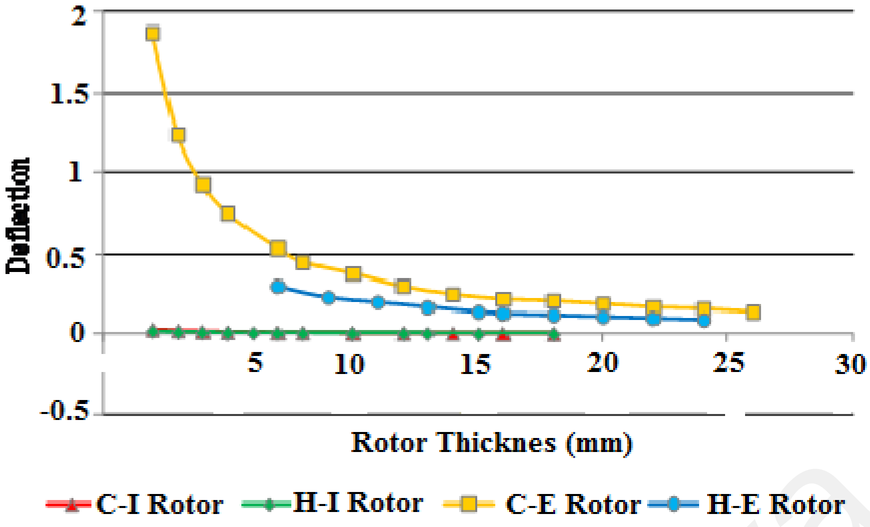

Figure 3.22: Mechanical deflection of rotor vs. rotor thickness (both in mm) for four different topologies

It is evident that deflection is higher in non-ferromagnetic rotor compared with ferromagnetic material. Thus, to ensure the deflection is within the acceptable range, the thickness of non-ferromagnetic rotor should be greater than that of the ferromagnetic one. According to Figure, the thickness of 8.0 mm and 4.0 mm is chosen for C-I and H-I Rotor respectively that comes with negligible deflection values which is 10% of allowable bending. On the other hand, with the maximum allowed deflection of 0.2 mm, the thickness of the C-E and H-E Rotor are selected to be 18 and 10 mm, respectively, which is safe bending for the epoxy rotors.

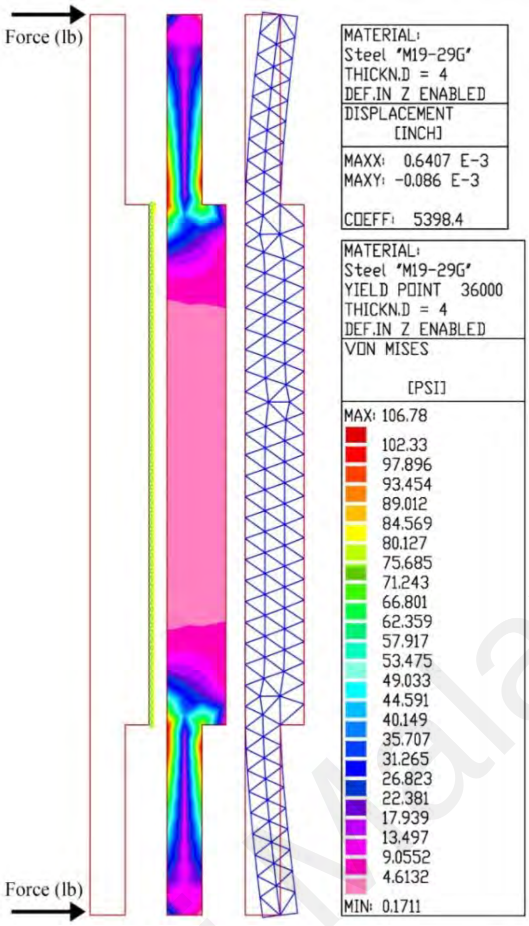

Figure3.23: Stress test results using von Mises' method in AutoCAD Mechanical for 4 mm C-I Rotor

3.5 Modeling of Multi-stage Coreless AFPM generator

Multistage coreless AFPM generator can be based on double-stator single-rotor (DSSR) or single-stator double-rotor (SSDR) configurations (Caricchi et al., 1996). Here, the single-stage configuration from chapter 4 is selected, where N-stage multi-stage machine will have N stators and (N+1) rotors. For the purpose of discussion in this paper, a two-stage (N=2) multi-stage machine is considered.

3.5.1 Conventional Direct Cascade Topology

The simplest form of multi-stage coreless AFPM generator is to directly cascade two or more single-stage AFPM machine together (Kahourzade et al., 2014). For example, two sets of single-stage machines can be simply combined to yield a multi-stage to increase the torque/power while maintaining the machine's diameter. As illustrated in the left column of Table 1.1, the direct cascade multi-stage AFPM has 2 stators and effectively 3 rotors (2 external rotors and 1 internal rotor). Due to direct cascading, the internal rotor is essentially back-to-back rotors of a single-stage generator. The stator coils are single layer concentrated windings of trapezoidal geometry which are embedded in epoxy and covered with composite material hardener to ensure enough mechanical strength. Based on analysis of single-stage coreless AFPM with C-I Rotor is used as the basic machine for comparison. Multi-stage version of the machine can be obtained by directly cascading two of these machines, which is regarded as conventional multi-stage coreless AFPM generator.

3.5.2 Proposed Hybrid Multi-Stage Coreless AFPM Topology

A hybrid multi-stage coreless AFPM generator is proposed where the iron rotors are replaced with epoxy rotors to improve the torque and power density. There are two significant modifications to the conventional direct cascade multi-stage coreless AFPM generator:

1. Halbach arrays are used on the external rotors to avoid leakage flux toward the exterior of the machine.
2. The back-to-back internal rotors are combined into a single internal epoxy rotor with conventional magnet array to simplify design and save materials

This proposed topology is a hybrid structure of the C-E and H-E Rotors presented in this section. By analyzing the flux path, it can be observed that the proposed topology retains similar path with the conventional direct cascade multi-stage coreless AFPM generator machine. However, the proposed topology is more compact and has lower weight due to the elimination of the back iron on the rotor. The magnet volume is kept constant as previous direct cascaded multi-stage coreless AFPM, by adjusting the magnet thickness of each rotor disc. Hence the thickness of the magnets of two external

Universiti Malaya

discs rotor and the thickness of the magnets of internal rotor are same whereas the total number of magnets are increased here from previous direct

Table 3.1: Different views of the two machine topologies

Conventional multi-stage coreless AFPM	**Proposed multi-stage coreless AFPM**
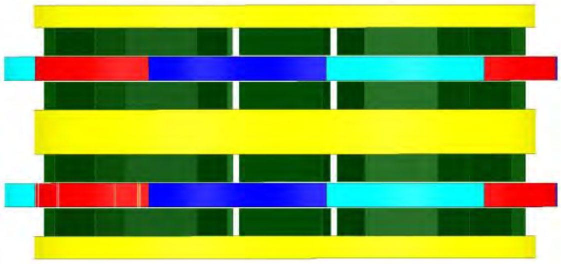 Complete model for axial length	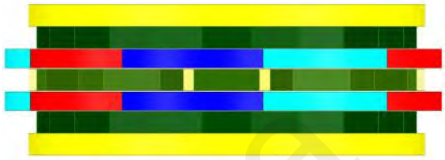 Complete model for axial length
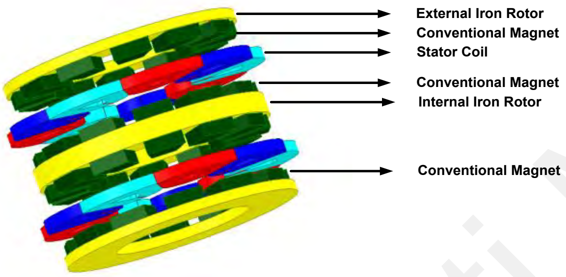 Whole model for different parts	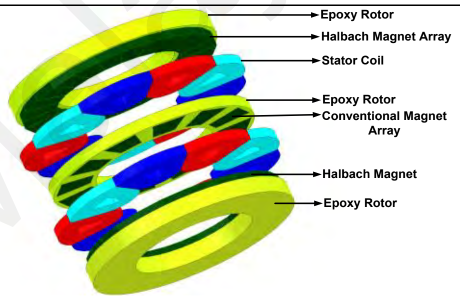 Whole model for different parts
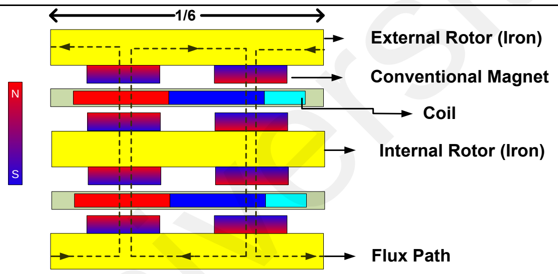 Flux Path	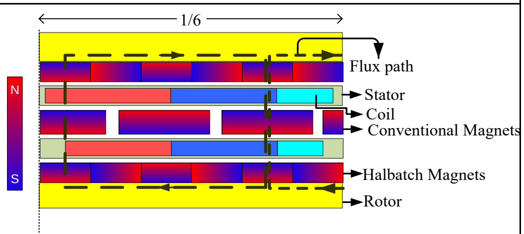 Flux Path

Cascade multi-stage coreless AFPM. Figure shows the difference between the external rotor and internal rotor of the proposed hybrid multi-stage coreless AFPM generator. The rotor structure is formed by trapezoidal shape magnets, rotor core, and shaft. The gap between the rotor and stator are kept at 0.5 mm on both sides. For stator part, the proposed topology maintains the same stator coil numbers, windings layout and geometry used in the direct cascade multi-stage coreless AFPM generator.

Universiti Malaya

In addition, the current loading for the stator coil is fixed here in order to get the performance of the modified rotor design. To make a fair comparison with the direct cascade multi-stage coreless AFPM generator, a fixed stator current of 5.23A_{peak} is considered here based on the stator wire gauge, which is AWG16. Figure5 represents the different load resistance for both multi-stage coreless AFPM generators with a fixed current loading. As the two different magnet arrangements (Halbach and conventional) are used in the design, the proposed machine is named as hybrid multi-stage coreless AFPM generator. The generator is designed with 12 poles, and 18 coils (both stators) for a speed of 500 rpm at 50Hz. Cross-sectional view of the proposed topology is shown in Figure, for better understanding of the design.

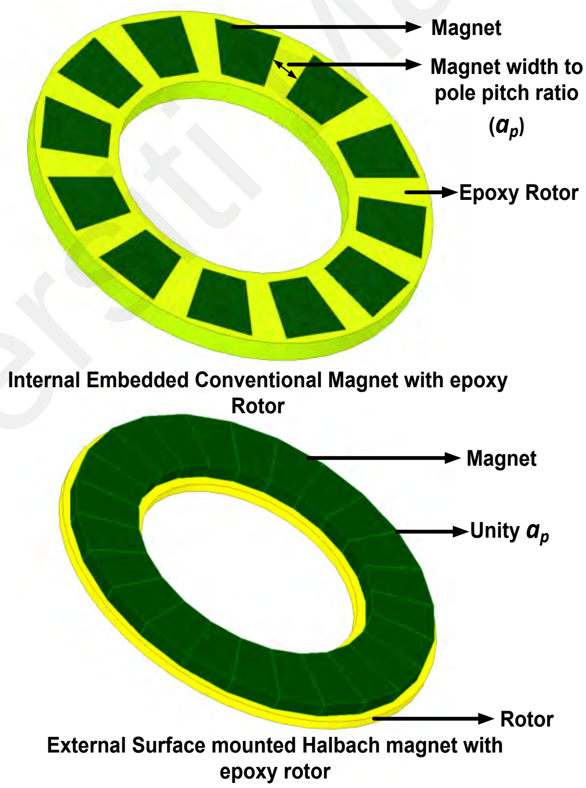

Figure 3.24: Schematic of internal and external rotor with conventional and Halbach magnet arrays

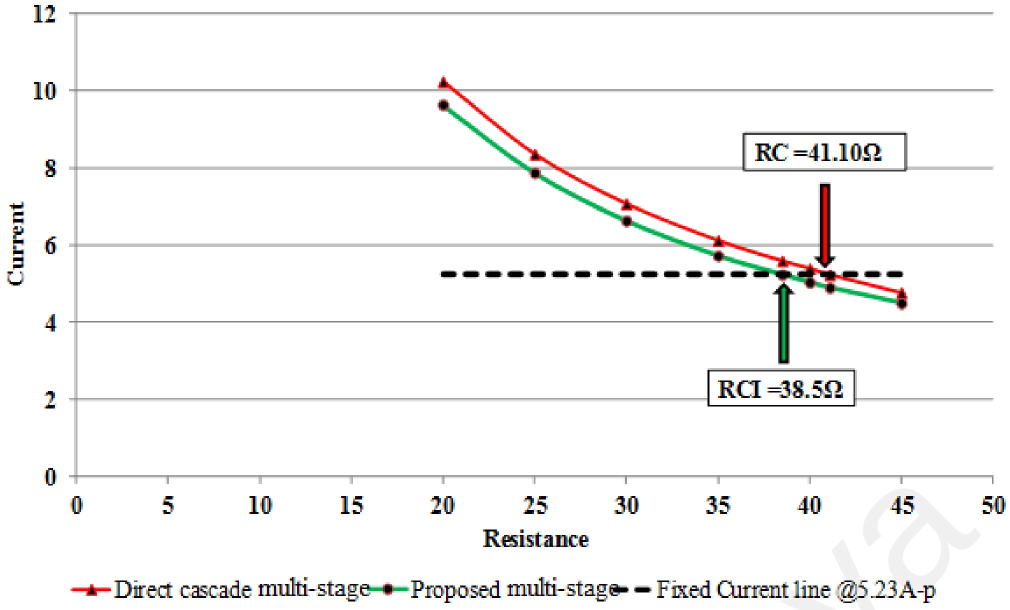

Figure 3.25: Resistive load of different multi-stage coreless AFPM for a fixed stator current

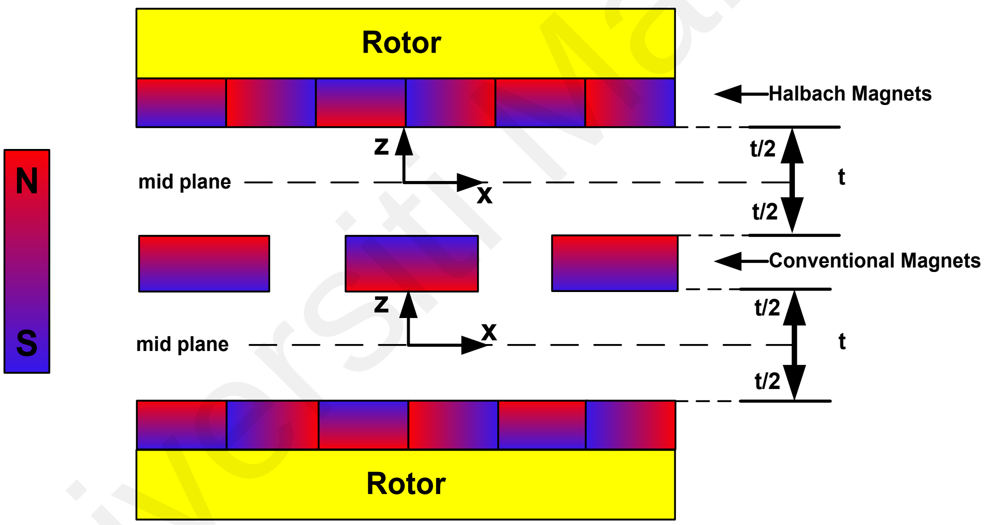

Figure 3.26: Plane region for the proposed hybrid multi-stage coreless AFPM generator

Universiti Malaya

CHAPTER 4: PERFORMANCE COMPARISION OF SINGLE-STAGE CORELESS AFPM GENERATORS WITH DIFFERENT ROTOR STRUCTURES

4.1 Introduction

It is interesting to compare performances of single-stage coreless AFPM generator using combinations of conventional and Halbach magnets with iron and non-iron (epoxy) rotor. For this purpose, a relatively lower speed of 500 rpm has been chosen that will reduce the number of poles which in turn alleviate the design and fabrication complexity. The comparative study has been carried out in terms of torque, torque ripple, voltage, current, power, weight and power density. In order to ensure a fair comparison, all the topologies are designed with same stator structure, machine diameter and volume of magnets. All the topologies designed with the same analytical equation validated with 3D finite element analysis (FEA) software ANSYS® Maxwell. Performance comparison of different types of single-stage coreless AFPM has discussed briefly in this chapter.

The common input parameters for the four topologies are shown in Table 4.1. Simulations are performed for all four generators which come with optimized rotor thickness in accordance with magnetic flux density B_g, leakage flux and the rotor mechanical deflection. From the FEA results the magnetic flux density in the air-gap, voltage, current, torque is taken as output results for ranking the performance of every single generator. Figure 4.1 and Figure 4.2 show the voltage and FFT analysis of the voltage. From the FFT analysis, the amplitude of the voltage is seen for the four different generators which are matched with the voltage waveform.

Universiti Malaya

Table 4.1: Common input parameters for all four topologies

		Parameter Name	Unit	Value
Input Parameters	General parameters	Number of Pole (P)	-	12
		Number of Coil (C)	-	9
		Rotational Speed (ω)	rpm	500
		No of Turn per Coil (N_C)	-	250
		Load Resistance	Ω	23
		Efficiency	η	94%
	Geometrical parameters	Ratio of Inner & Outer diameter (λ)	-	0.577
		Outer Diameter (D_o)	mm	180
		Inner Diameter (D_i)	mm	104
		Magnet Length (M_L)	mm	30
		Total Magnet Volume (M_V)	mm^3	$176.652e^3$
		Coil Axial thickness (C_h)	mm	8.5
		Coil Bandwidth (C_{BW})	mm	17

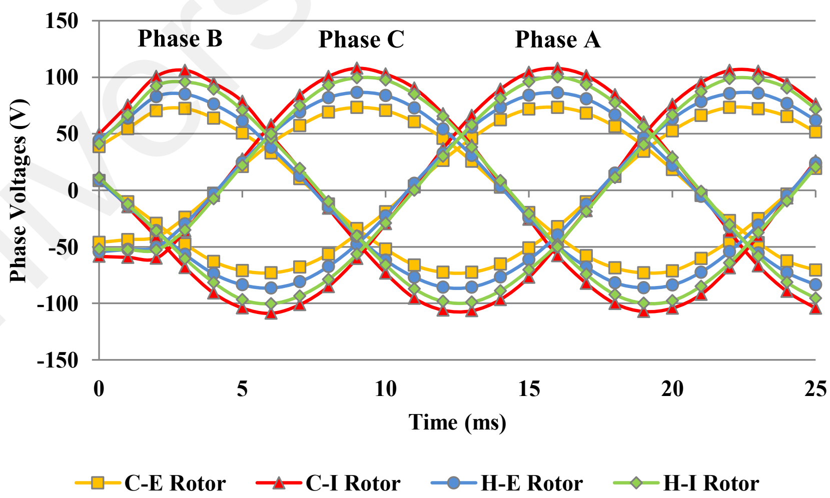

Figure 4.1: Voltage waveforms from the FEA analysis for C-E Rotor, C-I Rotor, H-E Rotor and H-I Rotor

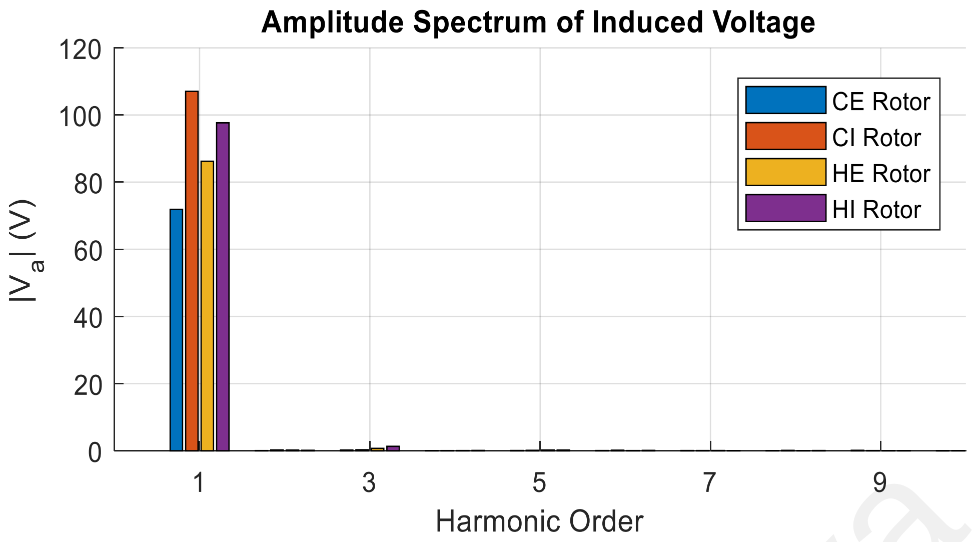

Figure 4.2: FFT analysis of induced voltage

Figure 4.3 and Figure 4.4 show the current, average torque and torque ripple for the four different single-stage AFPM generators: C-E Rotor, C-I Rotor, H-E Rotor and H-I Rotor. All the four generators are found to be able to deliver sinusoidal voltage and current which is expected from a three-phase generator.

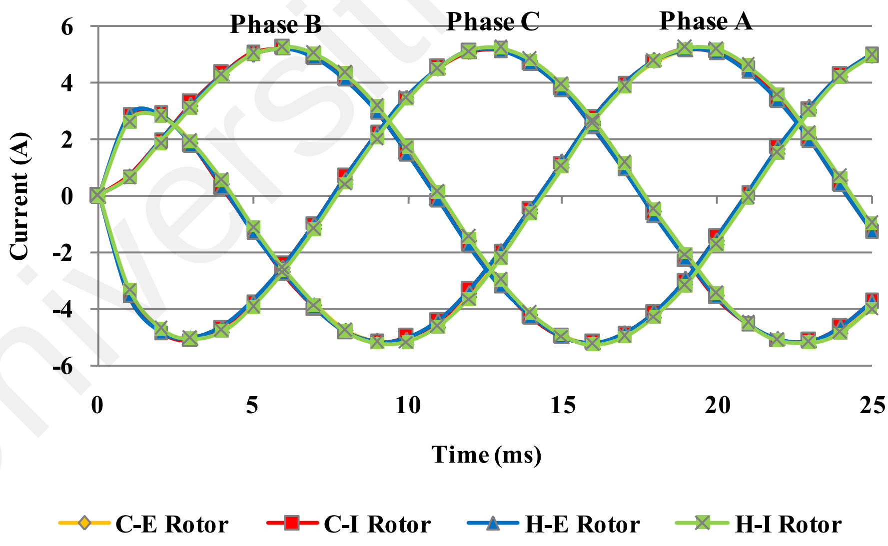

Figure 4.3: Current waveforms from the FEA analysis for C-E Rotor, C-I Rotor, H-E Rotor and H-I Rotor

Universiti Malaya

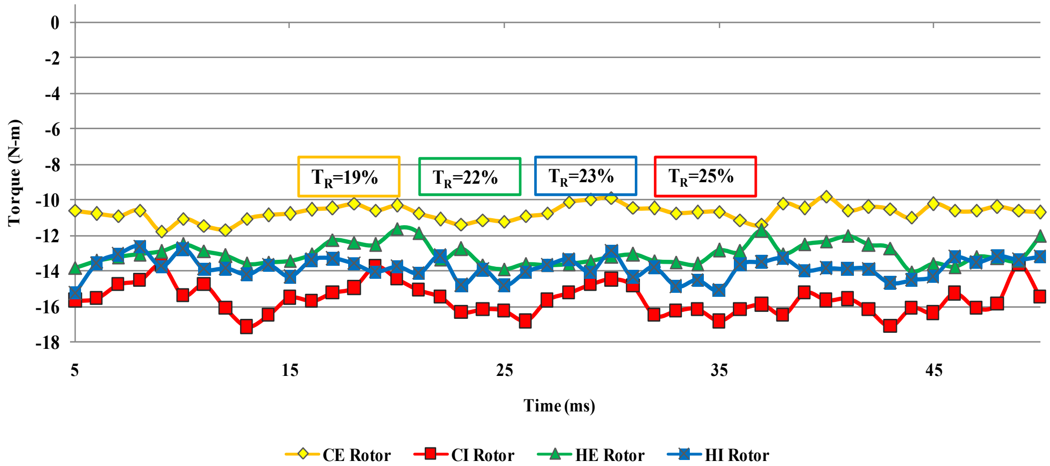

Figure 4.4: Average torque and torque ripple from the FEA analysis for C-E Rotor, C-I Rotor, H-E Rotor and H-I Rotor

4.2 Performance Comparison

The performance comparison of the four generators has been conducted based on few important output parameters, normally air-gap magnetic flux, average torque, torque ripple, power and power density. All the important output parameters are briefly described below for a comprehensive comparison.

4.2.1 Air-gap Magnetic Flux Comparison

Keeping the diameter, stator coil geometry and volume of magnets same for all the four different single-stage AFPM generators, it has been observed that each generator delivers different results shows all parameters and output values for the four generators.

Magnetic flux density B_g in the air-gap is the primary and most important parameter in machine design. Because the output power comes from the B_g, delivering from the magnets in a machine. Higher the amount of B_g creates higher the amount of power. In Figure 4.5, the comparison of B_g in the mid-plane of the air-gap of the two opposite rotors has been shown for the four different generators. From the figure it reveals that C-I Rotor has the highest B_g, leading to the highest power. This is followed by H-I Rotor, H-E Rotor and finally C-E Rotor. The C-I rotor is better than rotors with Halbach array because the optimum a_P enhance the magnetic flux and thereby increasing the B_g in the air-gap. However, if comparing the epoxy rotors, using Halbach array is better as it strengthens the air-gap flux and reduces the leakage flux. Table 4.2 shows comparisons among the four generators.

Table 4.2: Performance comparison among C-I, C-E, H-I and H-E Rotors

	Parameter	Unit	C-I Rotor	C-E Rotor	H-I Rotor	H-E Rotor
Geometrical Parameters	Magnet width to pole pitch ratio (α_p)	-	0.66	0.66	1.0	1.0
	Number of magnets (M_n)	-	12	12	24	24
	Magnet upper width (M_{WU})	mm	19.35	19.35	14.51	14.51
	Magnet lower width (M_{WL})	mm	29.72	29.72	22.364	22.364
	Load resistance	Ω	20.58	13.8	18.61	16.45
	Magnet axial thickness (M_h)	mm	10	10	6.654	6.654
Output Parameters and Simulation Results	Rotor thickness (R_t)	mm	8	18	4	10
	Total rotor weight	kg	0.527	0.03	0.38	0.01
	Total magnet weight	kg	1.32	1.32	1.32	1.32
	Stator coil weight	kg	1.57	1.57	1.57	1.57
	Total machine weight	kg	3.42	2.92	3.27	2.90
	Air-gap magnetic flux density (B_g)	T	0.7559	0.51	0.7018	0.59
	Peak voltage (V_{peak})	V	107.9	73.86	100.23	86.90
	RMS voltage (V_{rms})	V	76.3	52.22	70.87	61.44
	Peak current (I_{peak})	A	4.73	4.73	4.73	4.73
	RMS current (I_{rms})	A	3.7	3.7	3.7	3.7
	Average torque (T_{avg})	N-m	15.7	10.8	13.01	13.91
	Torque to current ratio	(N-m/A)	4.27	2.91	3.51	3.78
	Torque ripple (T_R)	%	25	19	23	22
	Power	W	822	565	728	681
	Power density	W/kg	240	194	222	235

Universiti Malaya

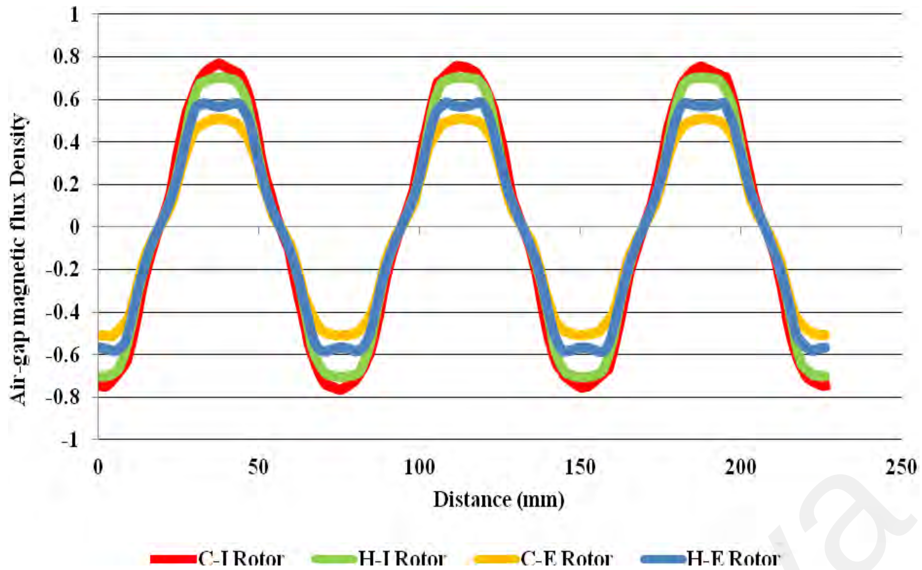

Figure 4.5: Magnetic flux density in the mid-level air gap for the four different generators

4.2.2 Torque and Torque Ripple Comparison

For designing a low speed single-stage coreless AFPM generator, torque quality is one big challenge. Torque ripples T_R are bound to create vibration and noise. In direct drive applications these vibrations transmitted directly to the load and drive shaft, which in return, affect the lifetime of the machine. Thus, a minimal torque ripple is important for AFPM generator. The torque ripples of the four different topologies can be seen in Figure 4.4 while the comparison is depicted in Figure 4.6. Though the C-E Rotor has the lowest torque ripple of 19%, its low average torque as well as low power density is not comparable with the other three machines. H-E Rotor has the second lowest torque ripple. From the FFT analysis of B_g, it can see easily the presence of 5th harmonics is the main cause of the ripple while 3rd harmonics is not present except the H-I Rotor. Figure 4.7 shows the amplitude spectrum of magnetic flux B_g.

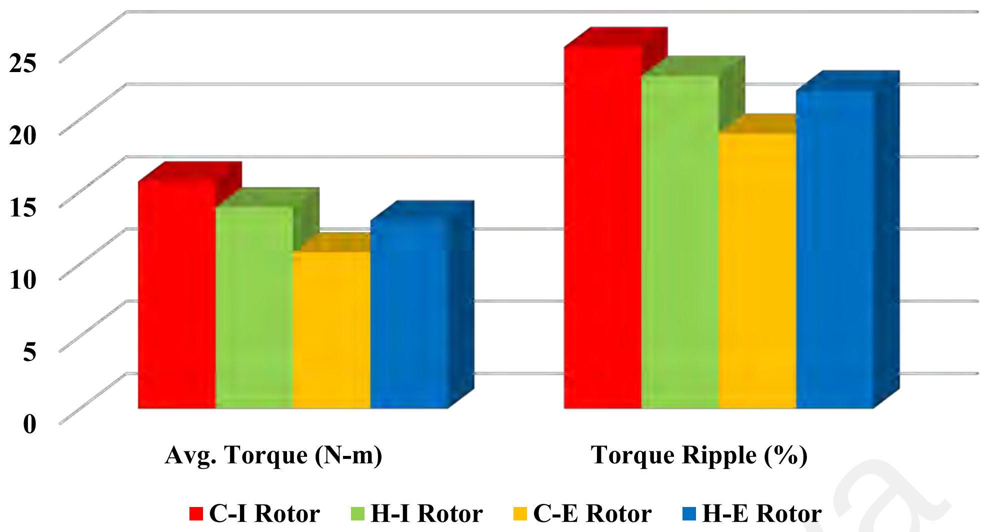

Figure 4.6: Comparison of average torque and torque ripple for the four different single-stage coreless AFPM generators

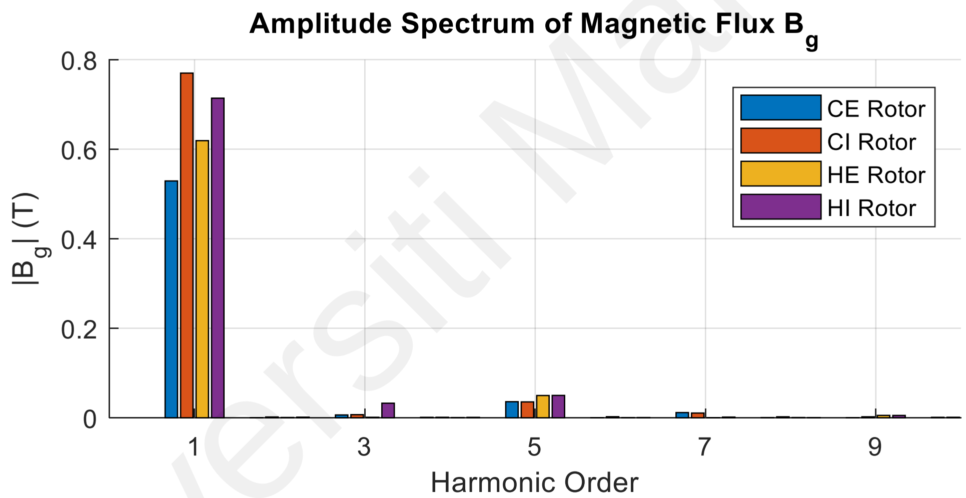

Figure 4.7: FFT analysis of the magnetic flux B_g

4.2.3 Power and Power Density Comparison

Although all the generators have the same magnet volume and same machine geometry, their performance varies according to different magnets arrangement and different rotor materials. The final output power and power density for the four machines are compared as shown in Table 4.2 and further illustrated in Figure 4.8. It can be seen that the C-I rotor delivers highest power at the highest power density. Although power delivered by H-I Rotor (728W) is 13% less than the C-I Rotor (822W), power density is only 5% less than the C-I Rotor generator. The C-E Rotor has the

Universiti Malaya

lowest power and power density with compared to the other three generators. Even though H-E Rotor gives the lower power (681W) than C-I rotor, it gives comparable power density, which is 2% less than the C-I Rotor. Therefore, it can be concluded that with a properly designed rotor, C-I Rotor is better than the other three topologies.

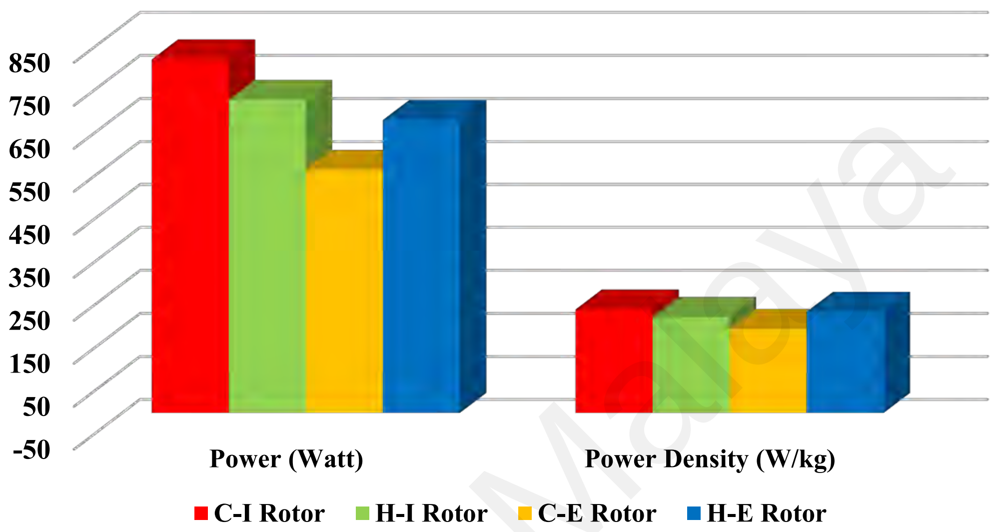

Figure 4.8: Comparison of power and power density for the four different generators

4.3 Cost Comparison

An approximated cost comparison among different single-stage coreless AFPM generators is presented in Table 4.3. In conducting the comparative cost analysis, exact cost of materials used in machine fabrication cannot be obtained, but indicative cost of machine is calculated based on the prices of the raw materials. only the prices of the active materials like mild steel, copper (RS, 2020) and plastic (Alibaba, 2020) of the generator have been taken into consideration. The comparison showed that the cost of the generators using epoxy rotor is lower than those with iron rotor by approximately 9%.

Universiti Malaya

Table 4.3: Cost comparison for the four different single-stage AFPM generators

Generator Name	Total rotor weight (kg)	Total cost of rotor ($)	Total magnet weight (kg)	Total cost of magnet ($)	Stator coil weight (kg)	Total Cost of Stator ($)	Total machine weight (kg)	Total cost of generator ($)
C-I Rotor	0.527	52.25	1.32	396	1.57	117.75	3.42	566
C-E Rotor	0.03	0.153	1.32	396	1.57	117.75	2.92	514
H-I Rotor	0.38	52.25	1.32	396	1.57	117.75	3.27	566
H-E Rotor	0.01	0.051	1.32	396	1.57	117.75	2.90	513

4.4 Summary

Design and performance comparison of single-stage coreless AFPM generator with different rotor structures have been discussed. Comparing the four different machines, the one with C-I Rotor is found to deliver the best performance. Although the full ironless AFPM generator using H-E Rotor provides less power than that C-I Rotor, power density of both machines is very much comparable. On the other hand, H-I Rotor gives slightly better power than H-E Rotor, but in terms of power density its performance is inferior. C-E Rotor produces the worst performance among all in terms of both power and power density. This shows that conventional magnet array is not suited for full ironless AFPM generator as expected.

Therefore, among the three machines other than C-I Rotor H-E Rotor is the best alternative. In addition to the benign feature offering almost the same power density as C-I Rotor with robust mechanical strength, the cost of H-E Rotor will be much lower as

Universiti Malaya

it is made of epoxy. Hence, this machine is technically rigorous as well as economically cost effective. Considering these advantages, AFPM generator with H-E rotor which is fully ironless, can be recommended for multi-stage coreless AFPM generator to cascade for having high power density with a limited diameter of the machine.

Universiti Malaya

CHAPTER 5: PERFORMANCE COMPARISON OFMULTI-STAGE CORELESS AFPM GENERATORSWITH DIFFERENT ROTOR STRUTURES

5.1 Introduction

This chapters presents the performance comparison of multi-stage coreless AFPM generator with different rotor structures, where multiple single-stage coreless AFPM generators are cascaded to increase overall power and torque. Instead of directly cascading the single-stage coreless AFPM generators, with either conventional magnet arrays or halbach array, a new hybrid structure is presented.The performance of the new multi-stage coreless AFPM with hybrid rotor is compared with multi-stage coreless AFPM based on direct cascading of single-stage coreless AFPM generators. The input parameters for the proposed and direct cascade design are shown in Table5.1.

5.2 Results and Performance Analysis

The two multi-stage generators are simulated using Ansys Maxwell FEA software. The results and performance of the proposed design are analyzed based on four important parameters, i.e. average torque, power, power density, and torque ripple. For analyzing the above parameters some fundamental parameters like magnetic flux density, voltage, current, FFT of voltage and magnetic flux are considered and present here. The simulated results for both magneto-static and transient are provided here for the better understanding and analyzing of the proposed design. Figure to Figure show all the magnetic flux density analysis from simulation results. Figure shows the flux density for the whole machine for both direct cascade and proposed multi-stage whereas in Figure shows the mid-air gap flux density for both set of internal and external rotors for proposed 'multi-stage coreless AFPM with hybrid rotor' and flux linkage to the stator coil is presented in Figure for direct cascade multi-stage coreless AFPM

Universiti Malaya

generator, and in Figure for proposed multi-stage coreless AFPM with hybrid rotor. The use of embedded conventional array magnets in the internal rotors makes sure a continuous flux path for the whole machine.

Table5.1: Input parameters for the proposed and direct cascaded multi-stage design

	Parameter Name	Unit	Direct Cascade Multi-stage	Proposed Multi-stage
General parameters	Number of pole (P)	-	12	
	Number of rotors		3	
	Number of coreless stators		2	
	Number of coils (C)	-	18	
	Rotational speed (N)	*rpm*	500	
	Number of turns per Coil (N_C)	-	250	
Specific design parameters	Ratio of inner &outer diameter (λ)	-	0.577	
	Outer diameter (D_o)	*mm*	180	
	Inner diameter (D_i)	*mm*	104	
	Air-gap between rotor & stator (t_g)	*mm*	0.5	
	Density of magnet (NdFeb)	g/cm^3	7.5	
	Iron density (steel M19G)	g/cm^3	7.4	
	Epoxy density	g/cm^3	1.25	
	Copper density	g/cm^3	8.96	
	Magnet length (M_L)	*mm*	30	
	Total magnet Volume (M_V)	mm^3	$353.3e^3$	
	Total magnet Weight	*kg*	2.6	
	Stator coil weight	*kg*	3.158	
	Stator epoxy weight	*kg*	$2.344e^{-4}$	
	Coil axial thickness (t_{Ch})	*mm*	8.5	
	Coil bandwidth (C_{BW})	*mm*	17	
	Conventional rotor thickness (t_{CR})	*mm*	8	

Universiti Malaya

Table 5.1, continued

	Parameter Name	Unit	Direct Cascade Multi-stage	Proposed Multi-stage
Specific design parameters	Halbach rotor thickness (t_{HR})	*mm*	10	10
	Modified rotor thickness (t_{Mod})		10	10
	Magnet width pole pitch ratio (a_P)	-	0.66 (C)	0.66(C) & 1(H)
	Number of magnet (M_n)	-	12×4 (C)	12×1(C) & 24×2(H)
	Magnet upper width (M_{WU})	*mm*	19.35 (C)	19.35(C) & 14.51(H)
	Magnet lower width (M_{WL})	*mm*	29.72 (C)	29.72(C) & 22.63(H)
	Magnet axial thickness (t_{Mh})	*mm*	10 (C)	10 (C) & 9.98(H)
	Total rotor weight	*kg*	1.074	0.1135
	Total weight of the generator	*kg*	6.83	5.87
	Total axial length of machine (T_L)	*mm*	$2\times(2t_{CR} + 2t_{Mh}$ (C). $+ 2t_g + t_{Ch}) =$ 91	$(2t_{HR} + 2t_{Mh}$ (H) $+ t_{Mod} + 4t_g + 2t_{Ch}) =$ 68.96
	Load Resistance	*Ω*	41.10	38.5

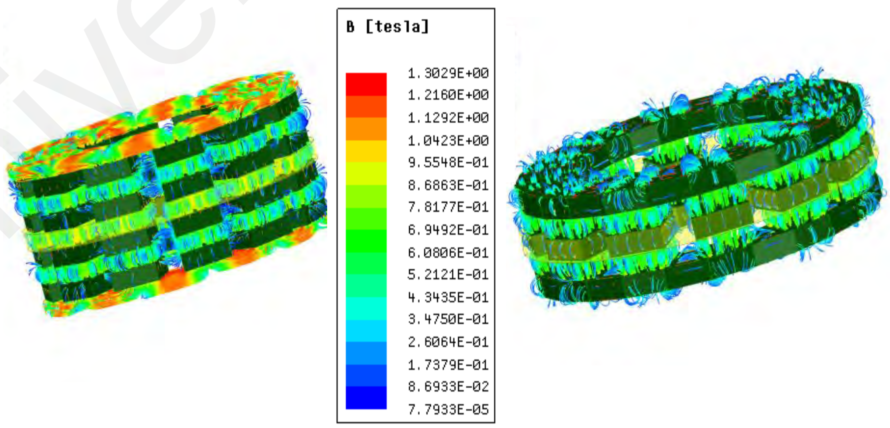

Figure 5.1: Simulated flux path for the conventional (left) and proposed (right) multi-stage AFPM generator (hiding the external rotor discs)

Universiti Malaya

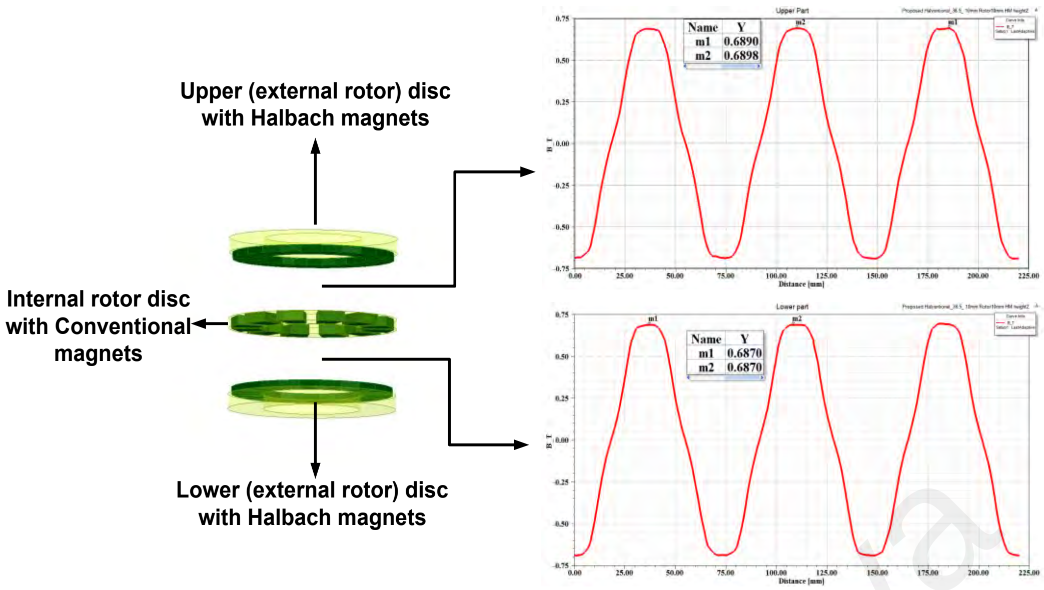

Figure 5.2: Air-gap magnetic flux density in the mid of air-gap between the internal and external rotors (proposed design)

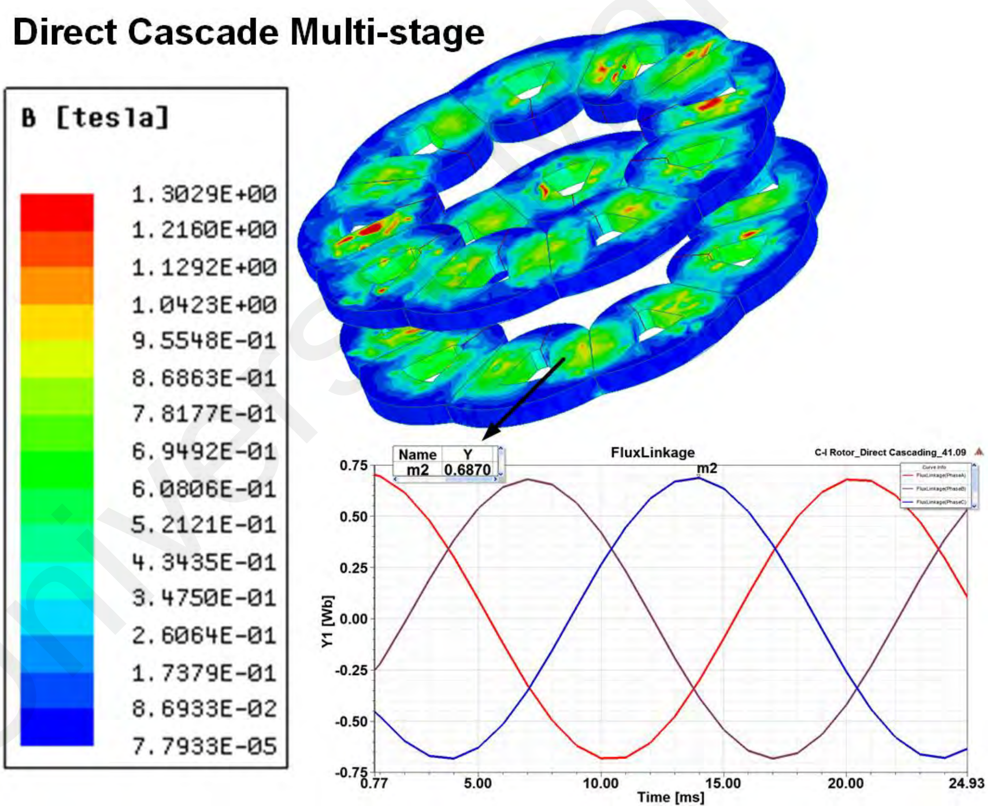

Figure 5.3: Magnetic flux density of the stator coils (flux linkage) for direct cascade multi-stage coreless AFPM generator

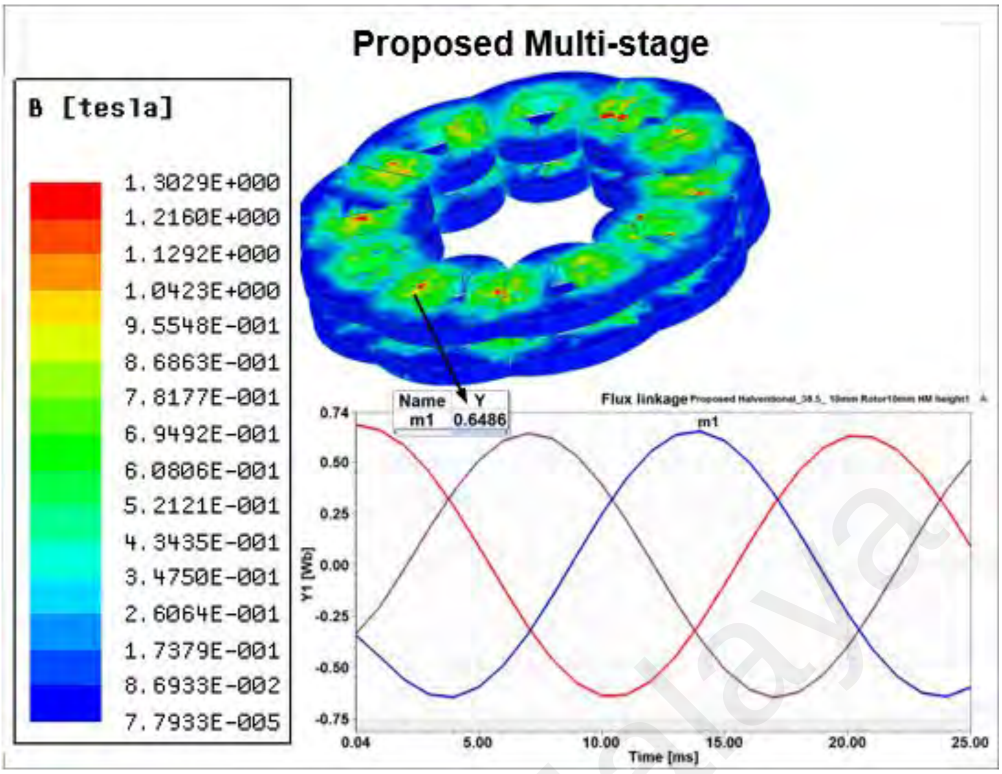

Figure 5.4: Magnetic flux density of the stator coils (flux linkage) for proposed multi-stage coreless AFPM with hybrid rotor

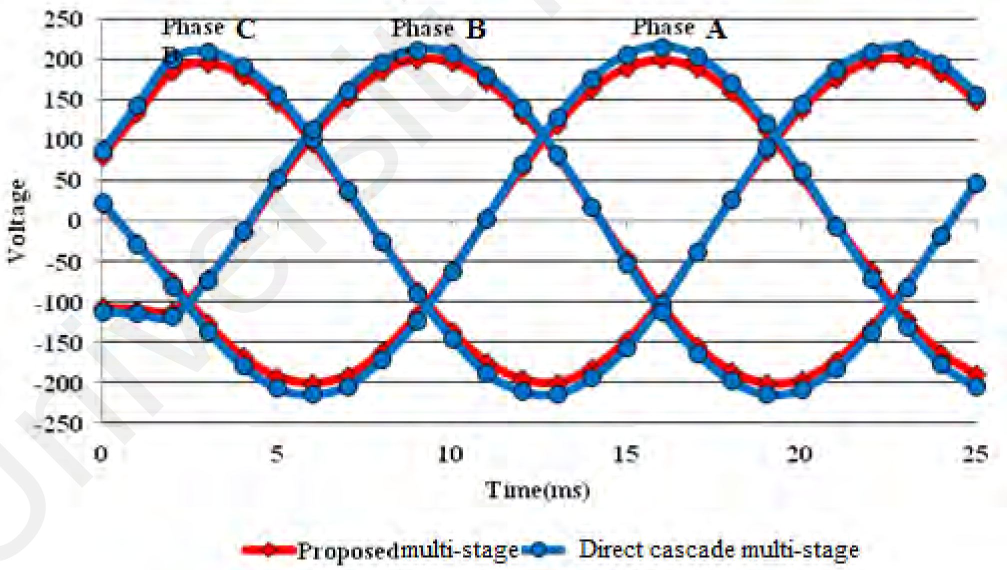

Figure to Figure show the voltage, current, average torque, and torque ripple (T_R) respectively for the both proposed and direct cascade multi-stage coreless AFPM generator. The proposed multi-stage coreless AFPM with hybrid rotor generator can deliver sinusoidal voltage and current like the direct cascade multi-stage coreless AFPM generator. This is required for a three-phase generator. Here it is important to mention that the current (Figure) is same for the both design as it was designed with same stator current loading. In terms of torque ripple, the proposed multi-stage coreless AFPM with hybrid rotor generator shows lower torque ripple of 13.2% compared to 18.6% in the direct cascade multi-stage coreless AFPM generator (Figure). Figure and Figure show the FFT of the magnetic flux density of the two machines. It can be concluded that the flux density is the direct cascade multi-stage coreless AFPM generator is higher which translate to higher voltage and torque generated. However, there is slightly higher 3rd and 7th harmonic current in the machine which can contribute to the higher torque ripple when compared to the proposed multi-stage coreless AFPM with hybrid rotor generator. Although the 5th harmonic in the proposed design is higher than the direct cascaded design, it cannot affect the torque ripple of the proposed design as the overall torque ripple reduction happened due to the lower 3rd and 7th harmonics. Table 5.2 shows the performance comparisons between the proposed multi-stage coreless AFPM with hybrid rotor generator with direct cascade multi-stage coreless AFPM generator which are further illustrated in Figure. The proposed multi-stage coreless AFPM with hybrid rotor generator offers higher power density, lower torque ripple and lower axial length of the whole generator. The higher power density comes basically from two important modification of the generator. The first one is the reduction of the internal rotor as well as one side of magnets and the second one is the combination of the Halbach and conventional magnets. The lower torque ripple comes for lower amplitude of the 5th harmonic, which is interacted with the fundamental harmonics. The reduced axial length of the machine is the cause of internal rotor modification as well as the elimination of the magnet array on one side.

Universiti Malaya

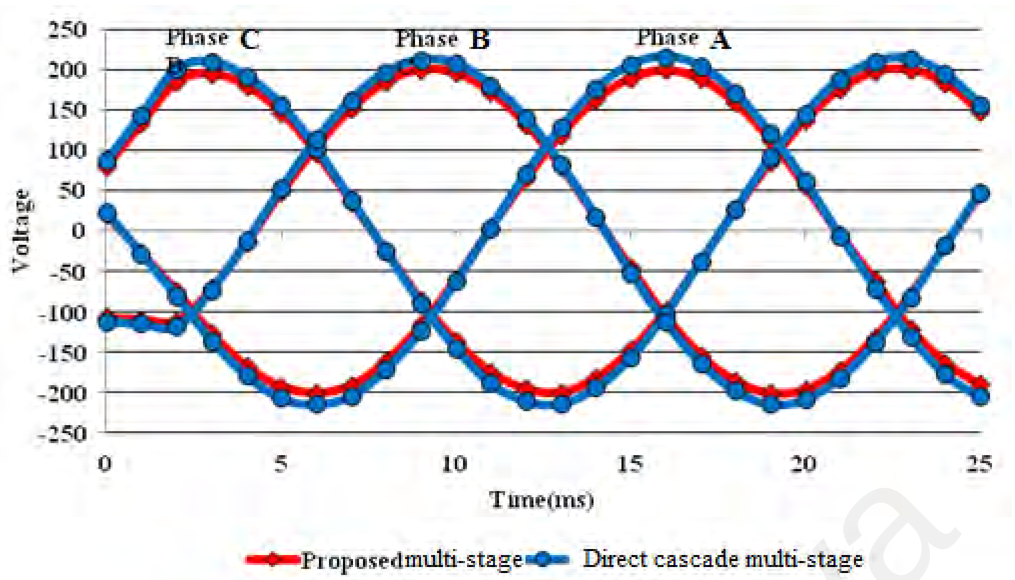

Figure 5.5: Voltage waveform for both the proposed and direct cascade multi-stage coreless AFPM generator from the FEA analysis

Table 5.2: Performance of the proposed multi-stage coreless AFPM with hybrid rotor generator

Machine Name	**Machine Weight (kg)**	**Power (W)**	**Power density (W/kg)**	**Average torque (τ_{avg})**	**Torque Density (Nm/kg)**	**Torque Ripple (TR)**
Direct cascade multi-stage	6.84	1659	242	31.69	4.63	18.6%
Proposed multi-stage	5.87	1510	257	28.85	4.91	13.2%

Universiti Malaya

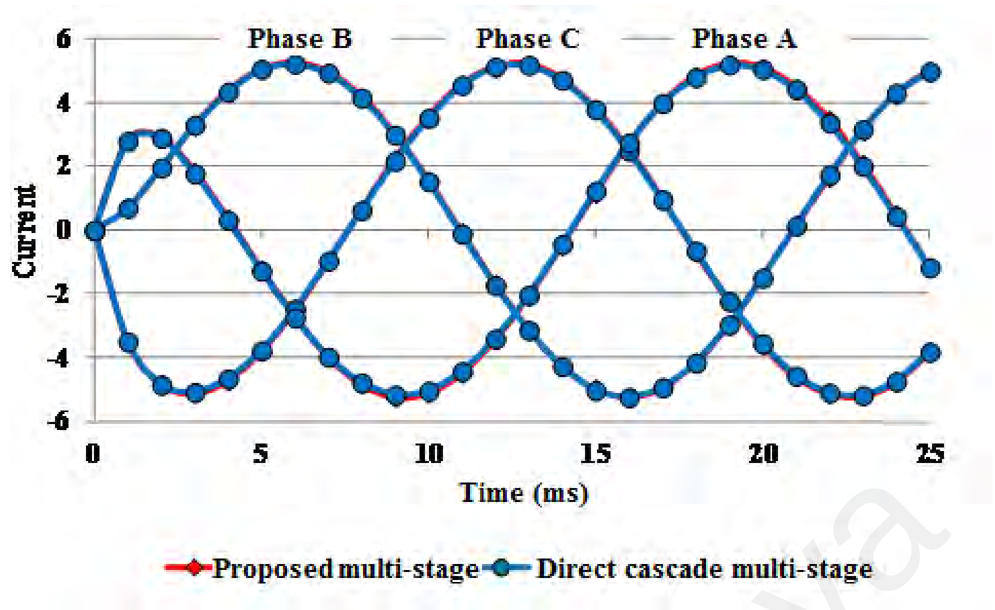

Figure 5.6: Current waveform for both proposed and direct cascade multi-stage AFPM from the FEA analysis

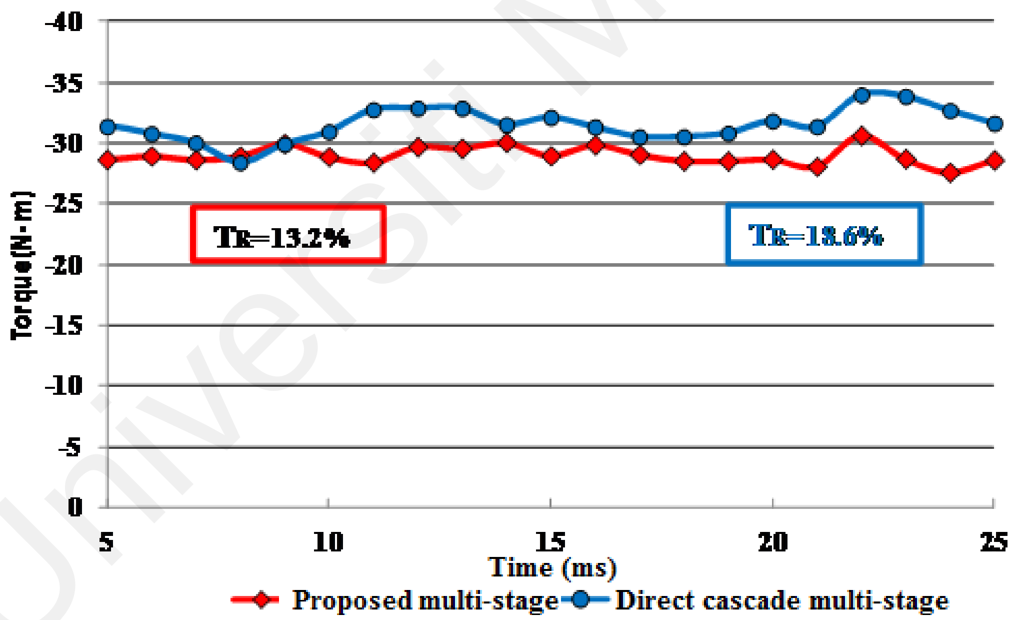

Figure 5.7: Torque waveform for both proposed and direct cascade multi-stage from FEA analysis

Universiti Malaya

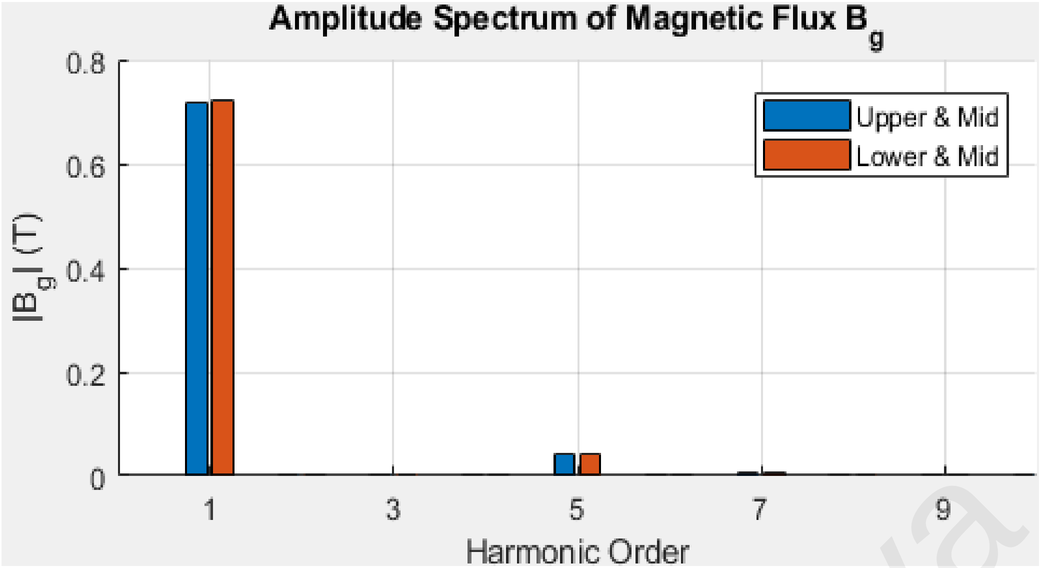

Figure 5.8: FFT analysis of magnetic flux density in the air-gap for both side of the internal rotor (proposed multi-stage)

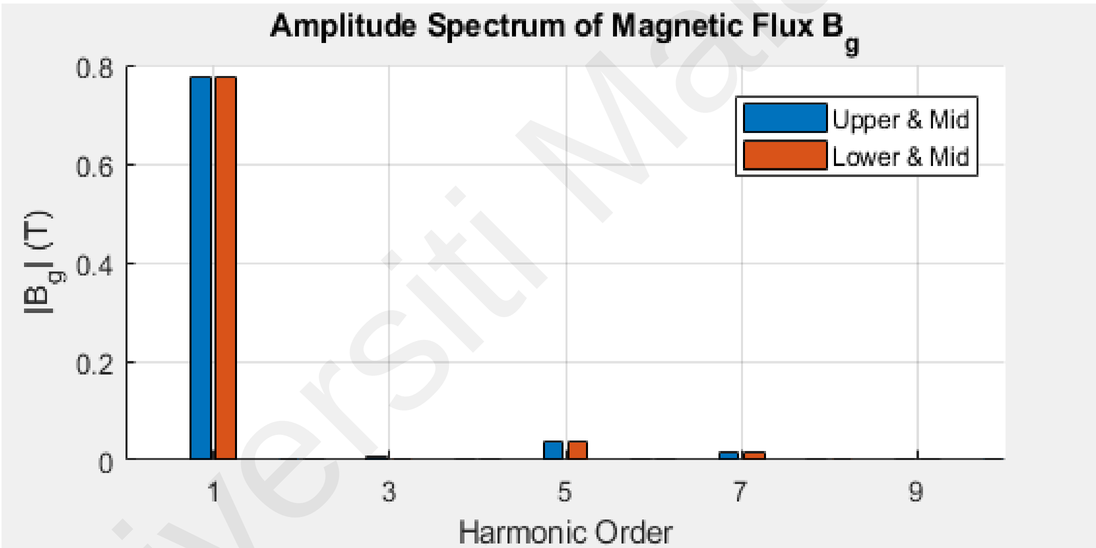

Figure 5.9: FFT analysis of magnetic flux density in the air-gap for both side of the internal rotor (direct cascade multi-stage)

Universiti Malaya

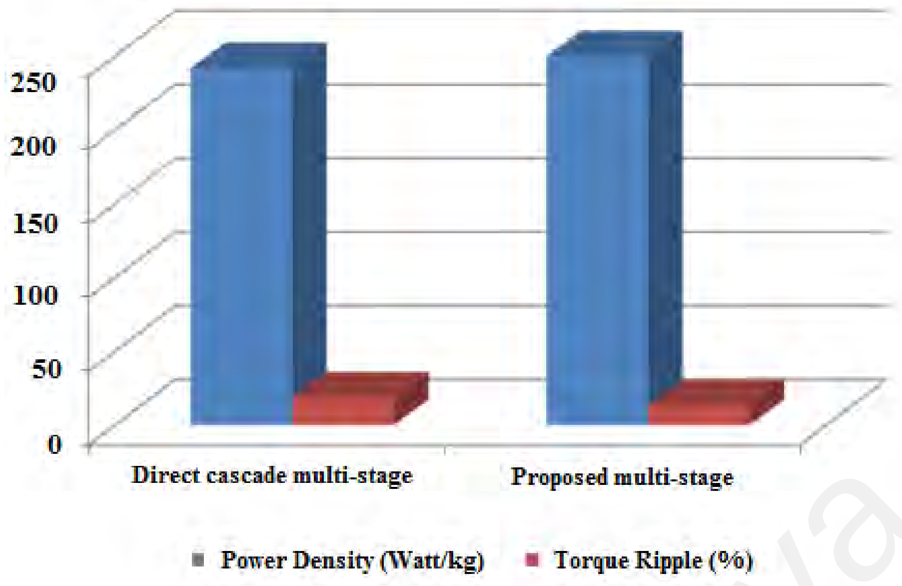

Figure 5.10: Performance comparison between direct cascaded multi-stage and proposed multi-stage coreless AFPM with hybrid rotor generator

5.3 Summary

In this chapter, the design and performance evaluation of multi-stage coreless AFPM with hybrid rotor generator has been presented. Cascading the full ironless machine in a modified manner the topology of multi-stage gives some performance improvements that can be recommended for AFPM generator. Several concluding remarks can be made in terms of performance analysis of multi-stage coreless AFPM generator:

1. A higher power density (6%) can be achieved by the proposed multi-stage coreless AFPM with hybrid rotor generator comparing the direct cascade multi-stage coreless AFPM generator.
2. A lower torque ripple can be obtained by this multi-stage topology.
3. Overall 24% axial length can be reduced by the design of proposed multi-stage coreless AFPM with hybrid rotor generator

CHAPTER 6: CONCLUSIONS AND RECOMMENDATIONS

6.1 Conclusions

In the present research, design and development of coreless AFPM generator have been made. Firstly, the comparative study of a single-stage coreless AFPM generator with through the four types of rotor is presented, where it was shown that fully-coreless AFPM generator with Halbach array has lower power and torque performance but comparable power density as conventional AFPM with iron rotor. Then, the concept of full ironless AFPM is extended for multi-stage coreless AFPM generator, where a modified topology is proposed. Using the modified structure, the proposed multi-stage coreless AFPM with hybrid rotor generatoris found to give better power density and low torque ripple. Detailed findings from these two aspects of the project are as enumerated in subsequent sections.

6.1.1 Single-stage Coreless AFPM Generator

A comparison of coreless AFPM generator with different rotor structures has been discussed in Chapter 4. These following points can be noted for the machines:

1. C-I Rotor has the best performance among the all four machines considering the power density. This is because of using iron rotor.
2. H-E Rotor is delivering the highest performance among the rest three. Even though the power is lower than C-I rotor, it gives comparable power density, which is only 2% less comparing to the C-I Rotor.
3. H-I Rotor gives slightly better power than H-E Rotor due to slight air-gap flux enhanced due to the use of iron rotor. However, in terms of power density, it is slightly poorer than the H-E Rotor, delivering 5% less power density and less

torque ripple (23%) compared to the C-I Rotor.

4. C-E Rotor has the worst performance which is 23% less power density than C-I Rotor and has the lowest torque ripple (19%) compared to the other machines. This highlights the importance of iron rotor when conventional magnet array is used.

Now, among the three machines only H-E Rotor is a feasible alternative to the normal C-I Rotor. Despite having a lower power, generator with H-E Rotor offers comparable power density, with an expected lower cost (cost of epoxy is generally lower than iron). Furthermore, H-E Rotor gives the less torque ripple by percentage. Considering these advantages, AFPM generator with H-E Rotor which is full ironless, can be recommended for multi-stage coreless AFPM generator to cascade for having high power density with a limited diameter of the machine.

6.1.2 Multi-stage Coreless AFPM Generator

In order to obtain higher power density, a new concept of full ironless multi-stage coreless AFPM with hybrid rotor generator has been discussed in chapter 5 of this thesis. Comparing the four different of single-stage machines, considered in chapter 4 C-I Rotor is delivering the best performance while H-E Rotor stood second. Despite having 2% less power density from C-I Rotor, generator of H-E Rotor offers comparable power density with lower torque ripple (22%) by percentage and expected lower cost (cost of epoxy is generally lower than iron). By cascading the H-E Rotor as well as replacing the middle (internal) rotor with C-E buried rotor to design multi-stage coreless AFPM with hybrid rotor, the performance of multi-stage AFPM is noticeably improved. The following points can be noted for the multi-stage coreless AFPM generator:

Universiti Malaya

1. The power density of the proposed multi-stage coreless AFPM with hybrid rotor generator is increased by 6% comparing to the direct cascading multi-stage.
2. The torque ripple reduced to 5.4% comparing to the direct cascading multi-stage.
3. The axial length of the proposed multi-stage coreless AFPM with hybrid rotor generator reduced significantly, which is 24%.

Considering these advantages, AFPM generator of multi-stage which is fully ironless/ coreless, can be recommended for application, where low power, low cost, robust and portable generator is necessary, such as wind/pico-hydro generator for rural electrification.

6.2 Contribution of the Present Research

The contributions of the present research project are:

1. Design and performance comparison of different single-stage coreless AFPM generators based on C-I, C-E, H-I, H-E Rotor.
2. Design and performance evaluation of a novel cascaded topology of AFPM generator comprising multi-stage coreless AFPM with hybrid generator combining both Halbach and conventional magnet arrays.

6.3 Recommendation for Future Works

Based on the findings from this project, there are some potential works which can be done in the future by extending the concepts presented in this thesis such as:

Universiti Malaya

(a) Experimental validation of the multi-stage coreless AFPM with hybrid generator

The application of the lower weight generator with a high-power density is necessary in wind and hydro power as it facilitated easy deployment. However, in order to ensure a higher power density generator, the design and simulation is fully done on this research work. The prototype of the design can be the future work to fully validate this simulated design.

(b) Extension of the multi-stage fully coreless AFPM generator design to machines with more than three phases

To get a higher power density machine multi-stage coreless AFPM with hybrid generator with multiphase idea is another interesting topic. Additional degrees of freedom in multi-phase machine can be used to inject higher order harmonics of current and enhance the torque producing capability of the machine. However, multi-stage AFPM with more than three phases would be the future work for an advanced research for developing AFPM machines.

Universiti Malaya

REFERENCES

Aydin, M., & Gulec, M. (2016). A new coreless axial flux interior permanent magnet synchronous motor with sinusoidal rotor segments. *IEEE Transactions on Magnetics, 52*(7), 1-4.

Alibaba (2020), Price of epoxy per kg, https://www.alibaba.com/showroom/price-of-plastic-per-kg.html, Accessed on June 2, 2202.

Aydin, M., Huang, S., & Lipo, T. A. (2006). Torque quality and comparison of internal and external rotor axial flux surface-magnet disc machines. *IEEE Transactions on Industrial Electronics, 53*(3), 822-830.

Campbell, P. (1974),*Principles of a permanent-magnet axial-field dc machine.* Paper presented at the Proceedings of the Institution of Electrical Engineers.

Caricchi, F., Crescimbini, F., Honorati, O., Bianco, G. L., & Santini, E. (1998). Performance of coreless-winding axial-flux permanent-magnet generator with power output at 400 Hz, 3000 r/min. *IEEE Transactions on Industry Applications, 34*(6), 1263-1269.

Caricchi, F., Crescimbini, F., Mezzetti, F., & Santini, E. (1996). Multistage axial-flux PM machine for wheel direct drive. *IEEE Transactions on Industry Applications, 32*(4), 882-888.

Caricchi, F., Crescimbini, F., & Santini, E. (1994),*Basic principle and design criteria of axial-flux PM machines having counter-rotating rotors.* Paper presented at the Proceedings of 1994 IEEE Industry Applications Society Annual Meeting.

Chan, T., & Lai, L. (2007). An axial-flux permanent-magnet synchronous generator for a direct-coupled wind-turbine system. *IEEE Transactions on energy conversion, 22*(1), 86-94.

Chan, T., Wang, W., & Lai, L. (2010). Performance of an axial-flux permanent magnet synchronous generator from 3-D finite-element analysis. *IEEE Transactions on energy conversion, 25*(3), 669-676.

Chirca, M., Breban, S., Oprea, C., & Radulescu, M. (2014),*Analysis of innovative design variations for double-sided coreless-stator axial-flux permanent-magnet generators in micro-wind power applications.* Paper presented at the 2014 International Conference on Electrical Machines (ICEM).

Universiti Malaya

Chung, D.-W., & You, Y.-M. (2014). Design and performance analysis of coreless axial-flux permanent-magnet generator for small wind turbines. *Journal of Magnetics, 19*(3), 273-281.

Daghigh, A., Javadi, H., & Torkaman, H. (2015),*Improved design of coreless axial flux permanent magnet synchronous generator with low active material cost.* Paper presented at the The 6th Power Electronics, Drive Systems & Technologies Conference (PEDSTC2015).

Daghigh, A., Javadi, H., & Torkaman, H. (2017). Optimal Design of Coreless Axial Flux Permanent Magnet Synchronous Generator with Reduced Cost Considering Improved PM Leakage Flux Model. *Electric Power Components and Systems, 45*(3), 264-278.

Davenport, T. (1837). Improvement in propelling machinery by magnetism and electro-magnetism. *US patent, 132*, 1836.

Eastham, J. F., Profumo, F., Tenconi, A., Hill-Cottingham, R., Coles, P., & Gianolio, G. (2002). Novel axial flux machine for aircraft drive: Design and modeling. *IEEE Transactions on Magnetics, 38*(5), 3003-3005.

Fei, W., Luk, P. C.-K., & Jinupun, K. (2010). Design and analysis of high-speed coreless axial flux permanent magnet generator with circular magnets and coils. *IET electric power applications, 4*(9), 739-747.

Gieras, J. F., Wang, R.-J., & Kamper, M. J. (2008). *Axial flux permanent magnet brushless machines*: Springer Science & Business Media.

Halbach, K. (1981). Physical and optical properties of rare earth cobalt magnets. *Nuclear Instruments and Methods in Physics Research, 187*(1), 109-117.

Halbach, K. (1985). Application of permanent magnets in accelerators and electron storage rings. *Journal of Applied Physics, 57*(8), 3605-3608.

Hosseini, S. M., Agha-Mirsalim, M., & Mirzaei, M. (2008). Design, prototyping, and analysis of a low cost axial-flux coreless permanent-magnet generator. *IEEE Transactions on Magnetics, 44*(1), 75-80.

Howard, J. (1967). Faraday, M-EXperimental Research in Electricity: Optical SOC Amer 2010 Massachusetts AVE NW, Washinton, DC 20036.

Huang, S., Aydin, M., & Lipo, T. A. (2001),*TORUS concept machines: pre-prototyping design assessment for two major topologies.* Paper presented at the Conference

Universiti Malaya

Record of the 2001 IEEE Industry Applications Conference. 36th IAS Annual Meeting (Cat. No. 01CH37248).

Huang, S., Luo, J., Leonardi, F., & Lipo, T. A. (1999). A comparison of power density for axial flux machines based on general purpose sizing equations. *IEEE Transactions on energy conversion, 14*(2), 185-192.

Javadi, S., & Mirsalim, M. (2008). A coreless axial-flux permanent-magnet generator for automotive applications. *IEEE Transactions on Magnetics, 44*(12), 4591-4598.

Javadi, S., & Mirsalim, M. (2010). Design and analysis of 42-V coreless axial-flux permanent-magnet generators for automotive applications. *IEEE Transactions on Magnetics, 46*(4), 1015-1023.

Kahourzade, S., Mahmoudi, A., Ping, H. W., & Uddin, M. N. (2014). A comprehensive review of axial-flux permanent-magnet machines. *Canadian Journal of Electrical and Computer Engineering, 37*(1), 19-33.

Kamper, M. J., Wang, R.-J., & Rossouw, F. G. (2008). Analysis and performance of axial flux permanent-magnet machine with air-cored nonoverlapping concentrated stator windings. *IEEE Transactions on Industry Applications, 44*(5), 1495-1504.

Kim, K.-C., Koo, D.-H., Hong, J.-P., & Lee, J. (2007). A study on the characteristics due to pole-arc to pole-pitch ratio and saliency to improve torque performance of IPMSM. *IEEE Transactions on Magnetics, 43*(6), 2516-2518.

Khan, S., Bukhari, S. S. H., & Ro, J. S. (2019). Design and Analysis of a 4-kW Two-Stack Coreless Axial Flux Permanent Magnet Synchronous Machine for Low-Speed Applications. *IEEE Access*, *7*, 173848-173854

Latoufis, K., Messinis, G., Kotsampopoulos, P., & Hatziargyriou, N. (2012). Axial flux permanent magnet generator design for low cost manufacturing of small wind turbines. *Wind engineering, 36*(4), 411-431.

Lee, D., Jeon, K., Kim, Y., & Jung, S. (2015),*Performance evaluation of coreless axial flux permanent magnet wind generator.* Paper presented at the 2015 IEEE International Magnetics Conference (INTERMAG).

Lee, M. G., Lee, S. Q., & Gweon, D.-G. (2004). Analysis of Halbach magnet array and its application to linear motor. *Mechatronics, 14*(1), 115-128.

Universiti Malaya

Mahmoudi, A., Kahourzade, S., Rahim, N. A., & Hew, W. P. (2013). Design, analysis, and prototyping of an axial-flux permanent magnet motor based on genetic algorithm and finite-element analysis. *IEEE Transactions on Magnetics, 49*(4), 1479-1492.

Martin, R. (2007). *Axial flux permanent magnet machines for direct drive applications.* Durham University.

Minaz, M. R., & Çelebi, M. (2017). Design and analysis of a new axial flux coreless PMSG with three rotors and double stators. *Results in Physics, 7*, 183-188.

Ofori-Tenkorrang, J., & Lang, J. (1995),*A comparative analysis of torque production in Halbach and conventional surface-mounted permanent-magnet synchronous motors.* Paper presented at the Industry Applications Conference, 1995. Thirtieth IAS Annual Meeting, IAS'95., Conference Record of the 1995 IEEE.

Parviainen, A., Niemela, M., & Pyrhonen, J. (2004). Modeling of axial flux permanent-magnet machines. *IEEE Transactions on Industry Applications, 40*(5), 1333-1340.

Praveen, R., Ravichandran, M., Achari, V. S., Raj, V. J., Madhu, G., & Bindu, G. (2012). A novel slotless Halbach-array permanent-magnet brushless dc motor for spacecraft applications. *IEEE Transactions on Industrial Electronics, 59*(9), 3553-3560.

QI, L.-x., WANG, X.-y., DU, J.-j., Fang, Z., & TANG, R.-y. (2006). Magnetic field analysis of disk coreless permanent magnet synchronous motor based on thickness variation Halbach array. *Journal of Iron and Steel Research, International, 13*, 439-443.

Rossouw, F. G. (2009). *Analysis and design of axial flux permanent magnet wind generator system for direct battery charging applications.* Stellenbosch: University of Stellenbosch.

RS (2020) Mild steel price per kg, https://my.rs-online.com/web/p/steel-angles/0770658?cm, Accessed on June 4, 2020.

Sadeghierad, M., Darabi, A., Lesani, H., & Monsef, H. (2009). Rotor yoke thickness of coreless high-speed axial-flux permanent magnet generator. *IEEE Transactions on Magnetics, 45*(4), 2032-2037.

Tan, Y., Shen, J.-X., Jin, M.-J., & Hao, H. (2015),*Study of magnet fatigue in hybrid PM memory motors.* Paper presented at the Sustainable Mobility Applications, Renewables and Technology (SMART), 2015 International Conference on.

Universiti Malaya

Ubani, O. G., Mueller, M. A., Chick, J., & McDonald, A. (2016). Analysis of an air-cored axial flux permanent magnet machine with Halbach array.

Upadhyay, P. R., & Rajagopal, K. (2006). FE analysis and computer-aided design of a sandwiched axial-flux permanent magnet brushless DC motor. *IEEE Transactions on Magnetics, 42*(10), 3401-3403.

Virtic, P., Pisek, P., Marcic, T., Hadziselimovic, M., & Stumberger, B. (2008). Analytical analysis of magnetic field and back electromotive force calculation of an axial-flux permanent magnet synchronous generator with coreless stator. *IEEE Transactions on Magnetics, 44*(11), 4333-4336.

Virtič, P., Vražić, M., & Papa, G. (2016). Design of an axial flux permanent magnet synchronous machine using analytical method and evolutionary optimization. *IEEE Transactions on energy conversion, 31*(1), 150-158.

Wang, R.-J., & Kamper, M. J. (2004). Calculation of eddy current loss in axial field permanent-magnet machine with coreless stator. *IEEE Transactions on energy conversion, 19*(3), 532-538.

Wang, W., Cheng, K., Ding, K., & Meng, L. (2011). A novel approach to the analysis of the axial-flux permanent-magnet generator with coreless stator supplying a rectifier load. *IEEE Transactions on Magnetics, 47*(10), 2391-2394.

Winter, O., Kral, C., & Schmidt, E. (2013),*Design and loss assessment of air cored axial flux permanent magnet machines.* Paper presented at the Electric Machines & Drives Conference (IEMDC), 2013 IEEE International.

Xia, B., Shen, J.-X., Luk, P. C.-K., & Fei, W. (2015). Comparative study of air-cored axial-flux permanent-magnet machines with different stator winding configurations. *IEEE Transactions on Industrial Electronics, 62*(2), 846-856.

Zhu, D., Beeby, S., Tudor, J., & Harris, N. (2013). Increasing output power of electromagnetic vibration energy harvesters using improved Halbach arrays. *Sensors and Actuators A: Physical, 203*, 11-19.

Zhu, Z., & Howe, D. (2001). Halbach permanent magnet machines and applications: a review. *IEE Proceedings-Electric Power Applications, 148*(4), 299-308.

University Malaya